universität wien

MASTERARBEIT / MASTER'S THESIS

Titel der Masterarbeit / Title of the Master's Thesis

„Characterization of the domesticated mammalian transposon protein L1TD1"

verfasst von / submitted by

Alexandra Podhornik, BSc

angestrebter akademischer Grad / in partial fulfilment of the requirements for the degree of

Master of Science (MSc)

Wien, 2023 / Vienna, 2023

Studienkennzahl lt. Studienblatt / degree programme code as it appears on the student record sheet:	UA 066 834
Studienrichtung lt. Studienblatt / degree programme as it appears on the student record:	Masterstudium Molekulare Biologie / Master in Molecular Biology
Betreut von / Supervisor:	ao. Univ.-Prof. Dr. Christian Seiser

Acknowledgments

At this point I would like to sincerely thank my supervisor, Christian Seiser, for not only giving me the opportunity to work in his lab but also for giving me active support and for answering all my upcoming questions during the process of my Master thesis.

Furthermore, I want to thank Gülnihal Kavaklioglu for being a teacher in the lab and a good friend outside of the office. Thank you for being such a kindhearted, calm and patient person, you took away my fear and made every day interesting and exciting for me. And an additional thank you for buying me lunch every time I was overwhelmed with experiments and work, you are a lifesaver!

I also want to thank Terezia Vcelkova for knowing where every protocol and every reagent and solution I ever looked for was.

A big thank you to my family, for always believing in me, for listening to me, for pushing me forward and especially for giving me the opportunity to study and to follow my dreams. Without you none of this would be possible.

Thank you also to my boyfriend and my close friends for listening to me when I again unstoppably talk about proteins, DNA and RNA, and for cheering me up when my experiments fail and when my motivation drops.

I also want to thank the rest of Christian Seiser's working group, thank you Natalija Cvetkovic, Lena Hess, Jelena Marjanovic, Heinz Fischer, Selina Knörzer and Valentina Stolz for being a great team that I certainly miss working with.

Abstract

Transposable elements (TE) make up more than 40% of the human genome. DNA transposons propagate themselves by a cut-and-past mechanism, while retrotransposons use a copy-and-paste mechanism called retrotransposition for their propagation and integration in the host genome. Due to these processes TEs endanger the integrity and function of the host genome. At the same time, TE activities can lead to evolutionary advantages and act as a resource for the formation of novel genes. Furthermore, host cells can domesticate TEs to use them for their own purposes. LINE-1 Transposase containing Domain 1 (L1TD1) is a domesticated TE protein, whose coding sequence is nearly entirely derived from the LINE-1 retrotransposon. Transposons are under the repressive control of cellular epigenetic mechanisms including DNA methylation. A previous study on L1TD1 has shown that its expression is also regulated by DNA methylation. Accordingly, we found that knockout of the maintenance DNA methyltransferase DNMT1 in the human cancer cell line HAP-1 led to derepression of L1TD1 expression, which is usually limited to a few tissues and undifferentiated cells. L1TD1 has been shown to have an important function in the maintenance of pluripotency of human embryonic stem cells but its mechanistic function in cancer cells is still unclear. This Master thesis focuses on the potential role of L1TD1 in the human cancer cell lines, OV-90 (ovarian cancer cells) and HAP-1 (cells derived from chronic myeloid leukemia cells).

The aim of this Master thesis was to investigate the potential regulatory role of L1TD1 as an RNA-binding protein in human cancer cells. In order to address this, HAP-1 cells expressing V5-tagged L1TD1 were generated using the CRISPR/Cas9 gene editing system in addition to DNMT1 KO and DNMT1/L1TD1 dKO HAP-1 cells. Since the L1TD1 protein has retained the RNA recognition motif from its ancestor gene LINE-1 ORF1p, we investigated its ability to act as an RNA-binding protein *via* RNA-immunoprecipitation experiments. Indirect immunofluorescence experiments demonstrated that L1TD1 is mainly localized to the cytosol where it partially co-localized with P-bodies, which indicates its potential role in RNA turnover. Moreover, we found out that L1TD1 might be a potential interaction partner of LINE-1 ORF1p. This interaction was demonstrated by co-immunoprecipitation experiments and immunofluorescence analysis. Mass spectrometry analysis of HAP-1 cells indicated that the loss of L1TD1 leads to a differential proteome in HAP-1 cells. Furthermore, an RNA-seq analysis showed a deregulated subset of genes in the absence of L1TD1.

In order to generate a similar system in OV-90 cells, an attempt was made to knockout/knockdown L1TD1 in this cell line. However, the attempts to knock-down and knockout L1TD1 in ovarian cancer cells failed probably due to its essential role in OV-90 cells. Our results overall show that L1TD1 binds to its own transcript and to other RNA targets. Its deletion results in a differential proteome and transcriptome in HAP-1 cells. Finally, we report an interaction of L1TD1 with its ancestor protein, LINE-1 ORF1p in the cytosol in both HAP-1 and OV-90 *via* immunofluorescence and co-immunoprecipitation experiments suggesting a regulatory role of L1TD1 on the function of LINE-1 retrotransposons.

Zusammenfassung

Repetitive Sequenzen wie Transposons machen mehr als 40% des menschlichen Genoms aus. DNA-Transposons vermehren sich innerhalb des Genoms mittels eines cut-and-past Mechanismus, während Retrotransposons einen copy-and-paste Mechanismus für ihre Vermehrung und Integration in das Wirtsgenom verwenden. Aufgrund dieser Prozesse stellen Transposons eine Gefahr für die Integrität und Funktion des Wirtsgenoms dar. Gleichzeitig kann die Aktivität von Transposons zu einem evolutionären Vorteil führen und die Ursache für die Bildung von neuen Genfunktionen darstellen. Weiters können Wirtszellen Transposons domestizieren und so ihre Funktion für ihre eigene Zwecke zu nutzen. LINE-1 Transposase containing Domain 1 (L1TD1) ist ein domestiziertes Transposonprotein, dessen kodierende Sequenz praktisch komplett von einem LINE-1 Retrotransposon abgeleitet ist. Transposons sind unter der repressiven Kontrolle von zellulären epigenetischen Mechanismen wie der DNA-Methylierung. Eine vorangegangene Studie hat gezeigt, dass die Expression von L1TD1 ebenfalls durch DNA-Methylierung reguliert wird. Dementsprechend konnten wir zeigen, dass der Knockout der Maintenance DNA Methyltransferase DNMT1 in der menschlichen Krebszelllinie HAP-1 zur Induktion der L1TD1-Expression, die normalerweise auf wenige Gewebe und undifferenzierte Zellen limitiert ist, führt. L1TD1 hat eine wichtige Funktion für die Aufrechterhaltung der Pluripotenz in menschlichen embryonalen Stammzellen, aber die mechanistische Funktion des Proteins ist noch nicht geklärt. Diese Masterarbeit beschäftigt sich mit der potenziellen Rolle von L1TD1 in den menschlichen Krebszelllinien OV-90 (Eierstockkrebszellen) und HAP-1 (Zellen, die von chronischer myeloischer Leukämie Zellen abgeleitet sind).

Das Ziel dieser Masterarbeit war es, die potentielle regulatorische Rolle von L1TD1 als RNA-bindendes Protein ist in menschlichen Krebszellen zu untersuchen. Zu diesem Zweck wurden mittels CRISPR/Cas9 Technologie HAP-1 Zellen, die V5-getaggtes L1TD1 exprimieren zusätzlich zu DNMT1-KO und DNMT1/L1TD1-dKO HAP-1 Zellen hergestellt. Da das L1TD1-Protein das RNA Recognition Motiv von seinem Vorgängerprotein LINE-1 ORF1p behalten hat, haben wir seine Funktion als RNA-binding Protein mittels RNA-Immunopräzipitationsexperimenten getestet. Indirekte Immunfluoreszenzexperimente zeigten, dass L1TD1 hauptsächlich im Zytosol lokalisiert ist, wo es mit P-Bodies kolokalisiert, was auf eine mögliche Rolle im RNA-Abbau hinweist. Weiters haben wir L1TD1 als potentiellen Interaktionspartner von LINE-1 ORF1p identifiziert. Diese Interaktion konnte durch Ko-Immunopräzipitationexperimente and Immunofluoreszenzanalyse nachgewiesen werden. Massenspektrometrieanalyse von HAP-1 Zellen zeigte, dass der Knockout von L1TD1 zu einer Änderung des Proteoms führt. Des Weiteren zeigte eine RNA-seq Analyse eine Deregulation des Transkriptoms in Abwesenheit von L1TD1. Um ein ähnliches experimentelles System in OV-90 Zellen herzustellen, haben wir versucht, L1TD1 in dieser Zelllinie mittels Knockout/Knockdown auszuschalten. Diese CRISPR-Cas9 und siRNA Experimente zeigten nicht den erwünschten Erfolg, was möglicherweise auf eine potentielle Abhängigkeit dieser Zellen von L1TD1 zurückzuführen ist. Zusammengefasst zeigen unsere Resultate, dass L1TD1 neben seinem eigenen Transkript ein Set von weiteren RNAs bindet. Knockout von L1TD1 resultiert in einer Veränderung des Proteoms and Transkriptoms in HAP-1 Zellen. Schließlich zeigen wir mittels Immunofluoreszenz und Ko-Immunopräzipitations-experimenten eine

Interaktion von L1TD1 mit seinem Vorgängerprotein LINE-1 ORF1p in HAP-1 und OV-90 Zellen. Dies weist auf eine regulatorische Rolle von L1TD1 für die Funktion von LINE-1 Retrotransposons hin.

Table of Contents

Abbreviations

APS Ammonium persulfate

DAPI 4', 6-diamino- 2-pheylindole

dKO Double knockout

hESCs Human embryotic stem cells

DMSO Dimethyl sulfoxide

EDTA Ethylenediaminetetraacetic acid

EtBr Ethidium bromide

EtOH Ethanol

ES Embryonic stem cell

FBS Fetal bovine serum

KO Knockout

KI Knockin

PBS Phosphate-buffered saline

PFA Paraformaldehyde

rcf Relative centrifugal force

rpm Revolutions per minute

TBS Tris-buffered saline

TEMED Tetramethylethylenediamine

TE Transposable element

n.d. no date

Introduction

1.2. Mobile elements in the human genome

Transposable elements (TEs) are omnipresent in almost all living beings, from prokaryotes to unicellular and multicellular eukaryotes and even in large DNA viruses. Transposable elements are parasitic DNA leftovers, their function was and still is to replicate and propagate themselves within the host genome (Muñoz-López, M., & García-Pérez, J. L. 2010). Transposable elements can be classified by their mobilization strategy whether they use an RNA (retrotransposon) or DNA (DNA transposon) based intermediate (Barrero, M. J. *et al.* 2020). They can additionally be classified by whether they encode proteins for their own mobility (autonomous) or are dependent on other elements within the host cell to help with these processes (non-autonomous), (Beck, C. R. *et al.* 2011). Autonomous transposons do not only copy themselves and change location on the chromosome, they can also move non-autonomous elements or even unrelated host gene sequences through the genome. To counteract an overflooding of these repetitive elements in the genome, many of these TE insertions are removed by a mechanism called purifying selection or are effectively neutral and fixed through genetic drift (Jangam, D. *et al.* 2017). Transposable elements do not only cause problematic mutations that would lead to different diseases, they can also be used and repurposed for cellular beneficial functions (Jangam, D. *et al.* 2017). This has been a quite important evolutionary step, especially for various defensive mechanisms against invasive genetic elements and other pathogens. A prime example of such an event is the V(D)J recombination system of jawed vertebrates. This conserved process creates an infinite repertoire of antibodies in their immune cells, leading to a fast and high response towards antigens expressed by pathogens. It was confirmed that an important protein, being involved in this process (RAG1) is a domesticated transposon (Jangam, D. *et al.* 2017).

Gene names	Ancestral TE	Originally discovered	Possible conflict	Function related to the conflict
Cas1	Casposon	Bacteria	Host vs. pathogen	Defense response to virus and maintenance of CRISPR repeat elements.
Cas9	DNA transposon	Bacteria	Host vs. pathogen	Integration of invading viral DNA into CRISPR locus.
L1TD1	**L1**	**Homo sapiens**	**TE vs. host**	**Potential role in TE control.**
PiggyMac	piggyBac	Paramecium tetraurelia	TE vs. host	Required for genome rearrangement in Paramecium tetraurelia.
RAG1	Transib	Homo sapiens	Host vs. pathogen	Important function in V(D)J combination and interacts with RAG2.
RAG2	Transib	Homo sapiens	Host vs. pathogen	Important function in V(D)J combination and interacts with RAG1.
Suppressyn	HERV-F	Homo sapiens	TE vs. host	Regulates syncytins and potential viral restriction into host cells.
Syncytin A, Syncytin B	HERV-F or HERV-H	Mus musculus	Fetus vs. mother	Placenta formation; fusogenic activities ex vivo.
TERT	LINE-like retroelement?	Homo sapiens	TE vs. host	RNA-directed DNA polymerase activity; telomerase RNA reverse transcriptase activity.

Figure 1 | Depiction of the most important domesticated transposon proteins and their functions. L1TD1 as a descendant of L1 (LINE-1) is highlighted in blue. Also, Cas9, a protein now widely used for genetic engineering came from a DNA transposon. Even Syncytin A and B, being involved in cell membrane fusion and placenta development are found on this protein set. Figure taken from *Jangam, D., Feschotte, C., & Betrán, E. 2017.*

Furthermore, there are other host proteins that are derived from the envelope genes (Env) of endogenous retroviruses. They are involved in the protection of the host against other related viruses, via blocking the entry of the virus by a process termed as receptor interference. Other proteins like the Gag proteins also share similar characteristics and restrict retroviral infections *(Jangam, D., Feschotte, C., & Betrán, E. 2017).* In **Figure 1***,* several of those virus defense genes are listed. Also the Cas9 protein, part of a now widely used method for genetic engineering, can be traced back to a DNA transposon. Cas9 is a bacterial endonuclease that cleaves DNA strands and is part of the bacteriophage defense system in bacteria. There are many other transposon derived genes, playing important roles in the eukaryotic genome and there will also be many more over time, since retrotransposition is still an ongoing process. For proper classification and understanding their mechanism of action, the structure of different mobile elements gets very important. Listed below in **Figure 2** is the structure, the percentage and the activity of DNA and RNA transposons in the human genome.

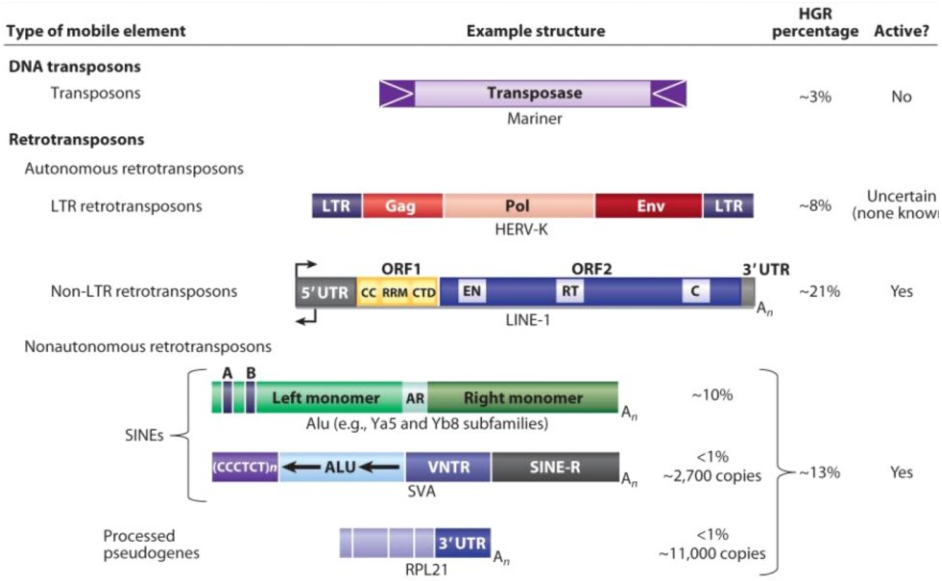

Figure 2 | Classes of mobile genetic elements present in the human genome. In this figure, the difference between the DNA transposon and retrotransposon structure and composition is depicted. It also shows their proportion and activity within the human genome. HGR: the human reference genome. Figure taken from *Beck, C. R. et al. 2011.*

DNA transposons usually move through the genome *via* a cut-and-paste mechanism. The transposons get excised out of their genomic location and are integrated somewhere else in the genome (*Muñoz-López, M., & García-Pérez, J. L. 2010*). They are flanked by two terminal inverted repeats (**Figure 2**), which are being recognized by the transposase. The transposase, a

cutting enzyme, cuts at these sites and the actual transposon DNA body gets inserted into a new location. As a consequence of this process the target site DNA is being duplicated after successful transposon insertion. This target site duplication is unique for each DNA transposon (*Muñoz-López, M., & García-Pérez, J. L. 2010*).

The process of retrotransposition is quite similar, except that the insertion of the DNA sequences is mediated by an RNA intermediate (*Ewing, A.D. et al. 2013*). With focus on the human genome, this process is carried out by the reverse transcriptase and endonuclease functions of the LINE-1 ORF2 protein, which additionally gets assisted by the LINE-1 ORF1 protein that facilitates RNA-binding (*Ewing, A.D. et al. 2013*).

To complete the transposition procedure, the DNA double strand breaks at the initial integration site of the transposon need to be repaired. To do this, many different repairing pathways are found.

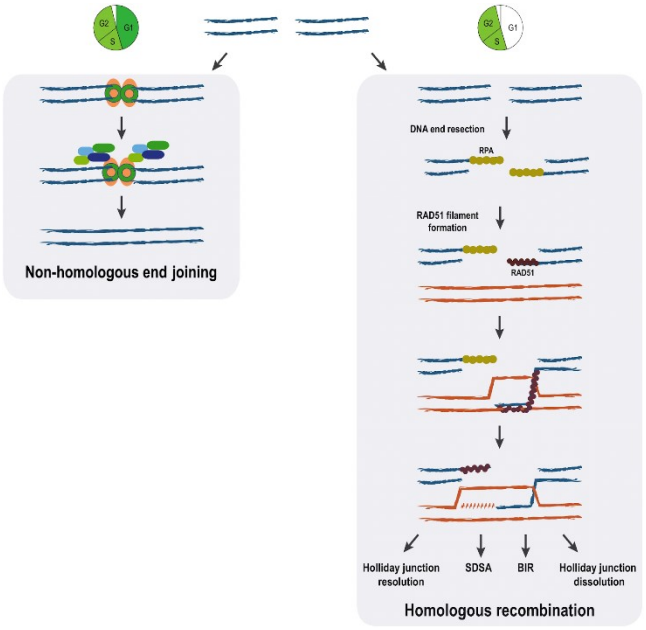

Figure 3 | Repair mechanisms after double strand breaks (DSB). To repair DSBs several mechanisms can be used. One way is the quick rejoining of the broken strand with no further processing, called the non-homologous end-joining (NHEJ). Another way works via using homologous sequences that are used as DNA templates (*Negritto, M. C. (n.d.)*). In both, several proteins are present assisting these mechanisms. Figure taken from *Vítor, A. C. et al. 2020*.

These repairing mechanisms can again highly differ in their execution. For example, the homologous recombination process can take place *via* the formation of Holliday junctions, by synthesis-dependent strand annealing (SDSA), the break-induced replication (BIR) or *via* the Holliday junction dissolution mechanism (*Constantinou, A. et al- 2002*). All of them share

identical initial steps but differ when it comes to the end joining step.
Even the cell cycle has an influence on the type of repair mechanism that is chosen (NHEJ or homologous recombination). The NHEJ is available during interphase, while homologous recombination is restricted to the S/G2 phases (*Vítor, A. C. et al. 2020*). The process of NHEJ can often lead to a subset of unfavorable mutations. A high amount of actively jumping transposons would thereby lead to an increased need of double strand break repair mechanisms. This would go hand in hand with an increased frequency of NHEJs.
Due to the increased mutation rate that is associated with NHEJ, mobile elements in the human genome can be linked to a variety of cancer types (*Anwar, S. L. et al. 2017*).

1.3. Transposable elements through evolution

Transposable elements are present in all organisms and around 46% of human DNA is derived from these transposons (*Pace, J. et al. 2007*). Their many nicknames like jumping genes, junk DNA or selfish DNA already indicates that there must be a huge controversy regarding their function.
Nowadays we know that these mobile and highly repetitive sequences can impact the mammalian genome in many ways. They can have different disruptive effects, for example by integration into regulator or coding regions, or by induction of ectopic/non-allelic recombination events *(Jangam, D. et al. 2017)*. Transposons can also serve as a genetic resource for the establishment of new and beneficial gene elements. They can help the immune system by using transposable elements from previous retroviral infections for the defense of other invading viruses *(Jangam, D. et al. 2017).* Together with a host defense mechanism, called purifying selection, the transposons can also be neutralized and give rise to non-replicative transposable elements *(Jangam, D. et al. 2017).*
In the 1950s, Barbara McClintock, an outstanding scientist working with maize as model organism, was the first to hypothesize the existence of genes that might move along the chromosomes. She observed that some genetic elements that were responsible for the cell color control of kernels, had the ability to change their location within the genome. This phenomenon had an influence on gene expression and phenotypic traits.
Since that eminent discovery other TEs like the P elements and I elements (important for the hybrid dysgenesis phenomenon) or gypsy (mdg4), Copia, and 412 in *Drosophila* were discovered (*Biémont, C. et al. 2010*).

In the 1990s the possible relationship between retroviruses and transposable elements was first considered. It was shown that TEs could produce virus-like particles and that their reverse transcriptase shared high similarity to those of retroviruses. Next, scientists tried to quantify these elements. After quantification they were surprised by their highly repetitive character (*Biémont, C. et al. 2010*).

Initially TEs were seen as useless junk DNA, as leftovers from different evolutionary steps. Now with their known power of invading genomes and populations, their influence on recombination rates, chromosomal rearrangements, mutation triggers and gene regulators, their highly important role was finally proven (*Biémont, C. et al. 2010*).

1.4. The epigenetics of transposable elements

Transposable elements are part of our genomes, but their quantity as well as their location are not predetermined from birth and can change within living organisms over time (*Underwood, C. J.et al. 2017*). Since transposons are mobile elements that upon activation can change location, their activity must be controlled. This happens via epigenetic modifications. Epigenetic modifications are reversible mechanisms that impact structure and function of the genome without interfering with the DNA sequence. Epigenetic mechanisms include DNA methylation and hydroxymethylation, histone modifications and regulation by microRNA species (*Misiak, B., Ricceri, L., Sąsiadek, M. M. 2019*). Important modifications that influence transposable elements are DNA methylation events. Since TEs make up more than 50% of the human genome and thereby contain around 52% of all CpG dinucleotides, which are the targets of this methylation process, the impact of methylation on the retrotransposon activity can't be denied. By measuring the methylation status of the TEs it was possible to estimate the global DNA methylation (Misiak, B., Ricceri, L., Sąsiadek, M. M. 2019).

Epigenetic mechanisms such as DNA methylation can also be used as a defense mechanism against transposable elements. By promoter methylation, the activity of the TEs can be dimmed (*Misiak, B., Ricceri, L., Sąsiadek, M. M. 2019*). Accordingly, it was shown that the majority of TEs in the human genome are hypermethylated (*Misiak, B., Ricceri, L., Sąsiadek, M. M. 2019*). Like it is with many other diseases, aberrant epigenetic regulations of TEs correlated with a higher susceptibility towards various mental disorders, like autism, schizophrenia, bipolar disorder, major depression, and Alzheimer's disease (*Misiak, B., Ricceri, L., Sąsiadek, M. M. 2019*).

The participation and upregulation of transposable elements in other diseases are positively linked to reduced methylation of their promoter regions, due to missing epigenetic modifications

(*Misiak, B., Ricceri, L., Sąsiadek, M. M. 2019*; *Xiao-Jie, L., et. al. 2016*). Especially in cancer and during brain development the cells showed an increased sensitivity to the regulatory effects of epigenetic mechanisms, which thereby more easily led to the enrichment of transposable elements (*Misiak, B., Ricceri, L., Sąsiadek, M. M. 2019*).

The abundance of mobile elements in the genome is therefore directly correlated to their epigenetic modifications (*Shapiro J. A. 2014*).

1.5. Retrotransposons

Since this study focuses primarily on RNA transposons only their propagation mechanism will be discussed in detail. Retrotransposons can again be subdivided into two groups, one where the transposable element is flanked by long terminal repeats, shortened the LTRs and one without them, the non-LTRs *(Cordaux, R., & Batzer, M. A., 2009).* The LTRs are endogenous retroviral remains and make up approximately 8% of the human genome. Most of the human TEs resulted from the activity of non-LTR retrotransposons. Some of the most known non-LTRs are the LINE-1 the Alu and the SVA elements, they make up nearly one third of the human genome and are also described as the only TEs being currently active in the genome *(Cordaux, R., & Batzer, M. A. 2009).*

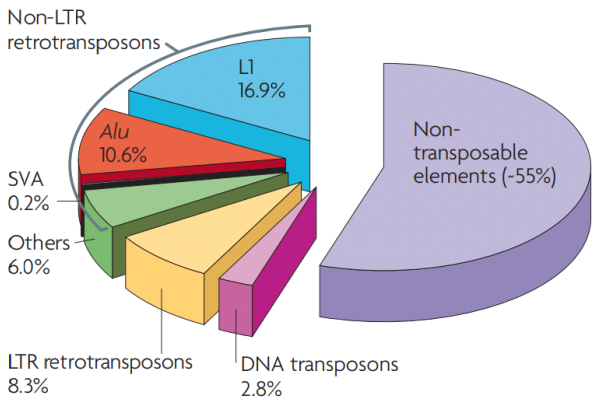

Figure 4 | Distribution of all transposable elements of the human genome. Around 45% of the human genome can be attributed to transposable elements such as LTRs and non-LTRs (LINE-1 (L1)), Alu, SVA elements). Only a small fraction are DNA transposons. Figure taken from *Cordaux, R., & Batzer, M. A. 2009.*

Non-LTR transposons are composed of long or short nuclear elements, the LINEs or SINEs (Alu SVA elements, LINE-1). LINE-1 is probably the best known and most characterized non-LTR element. It is 6-7kb long, contains a 5'UTR region with CpG islands, two open reading frames,

the ORF1 and ORF2 and a 3'UTR with a poly(A) sequence (**Figures 2** and **5**) *(Zhang, X. et al. 2020)*. SINE elements are only around 300 nucleotides long and contain an RNA polymerase III (Pol III) dependent promoter, they have no protein-coding capacity and are therefore relying on the activities of other retrotransposons *(Barrero, M. J. 2020)*.

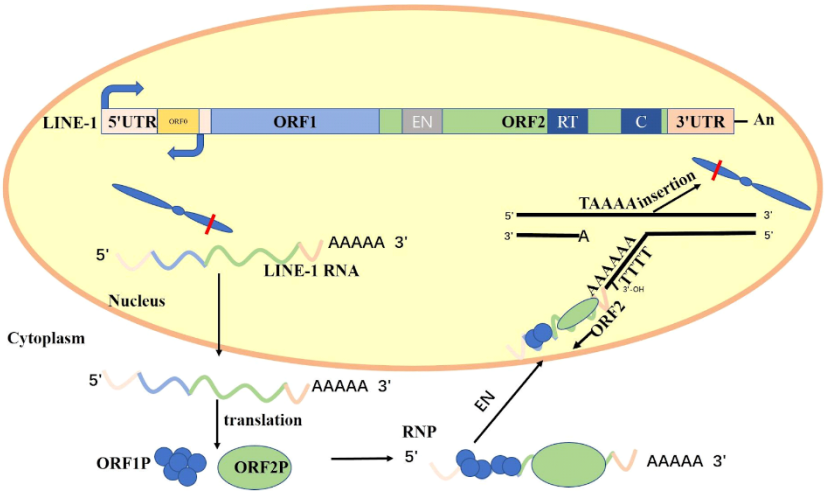

Figure 5 | Schematic view of the LINE-1 retrotransposition process. The 5'UTR harbors two internal promoters, one in sense and one in antisense. LINE-1 mRNAs that are transcribed from the sense promoter will be transported to the cytoplasm. Here they either are translated into ORF1p and ORF2p, or they become degraded or suppressed. Since the LINE-1 proteins have the capability to recognize and bind to their own transcript, they start to form so-called ribonucleoproteins (RNPs). This RNPs return to the nucleus where the mRNA gets reverse transcribed into cDNA and can be incorporated at different genomic locations *via* their endonuclease mechanism also called the target site-primed reverse transcription (TPRT) (*Xiao-Jie, L. et al. 2016*). Figure taken from *Zhang, X. et al. 2020.*

Their unique mechanism of invading the genome shouldn't be entirely seen as a cancer hallmark or a promoting effect of genomic instability. On the contrary, several studies have already shown that next to viral defense, retrotransposon activity can lead to the establishment of regulatory units that can be co-opted by the host cell (*Mita, P., & Boeke, J. D. 2016*). These transposon-derived regulatory features are widely distributed in the mammalian genome and again support the highly important role of retrotransposition during evolution (*Mita, P., & Boeke, J. D. 2016*).

1.6. LINE-1

LINE-1 (L1) as one of the most studied retrotransposons, as described in the paragraph above (*1.3. Retrotransposons);* makes up around ~17% of the human genome. *Via* its encoded proteins, ORF1p and ORF2p, it has the ability to mobilize non-autonomous retrotransposons, noncoding RNAs as well as messenger RNAs, leading to the emergence of new processed pseudogenes *(Beck, C. R. et. al. 2011)*. There are approximately ~8,000–15,000 processed pseudogene copies in the human genome. It was hypothesized that some mRNAs, like those coding for ribosomes, have a more efficient way to recruit LINE-1 encoded proteins. This would lead to an enriched occurrence of ribosomal pseudogenes which was already confirmed in the mammalian genome *(Beck, C. R. et. al. 2011)*. The LINE-1 TEs are the only known autonomously active human retrotransposons, even though over 99.9% of them have been inactivated by point mutations, inversions or truncations in the two encoded ORFs over time *(Beck, C. R. et. al. 2011).* Despite their downregulation, there are still full length retrotransposition-competent LINE-1 elements in the genome. After isolation of the LINE-1 progenitor genes, the presence of actively jumping LINE-1s was confirmed *(Beck, C. R. et al. 2011).* Furthermore, studies showed that new LINE-1 subfamilies form over time and start to replace older ones. A high amount of LINE-1 elements is shared between human and chimp genomes and probably represents a retrotransposition-defective molecular fossil *(Beck, C. R. et al. 2011).*

1.6.1. LINE-1 as a potential mutagen

Extensive data revealed that approximately 65 disease-causing mutations in humans can be attributed to LINE-1 mediated transposition events. Next to exon/splicing disruption, which will be discussed later (Figure 6), recent studies hypothesize that the LINE-1 endonuclease could also cause double strand breaks without the actual event of retrotransposition (Beck, C. R. *et al.* 2011). The investigation of LINE-1 as a potential hallmark of cancer and other immunological diseases has become more important over time. LINE-1 hypomethylation, especially in the LINE-1 promoter region, has been associated with genome-wide hypomethylation, which normally promotes chromosomal instability, genomic instability, and genetic heterogeneity. All these events are known to promote cancer development. In case of already present illnesses, the LINE-1 hypomethylation was reported to be associated with an overall poor survival in many different cancer types (Xiao-Jie, L., et. al. 2016). Through its copy-and-paste mechanism within the genome LINE-1 elements can also be integrated at undesired genomic locations, leading to

the activation of new oncogenes or the deletion of tumor suppressor genes. It was also shown that higher LINE-1 levels were associated with poor blood sugar and lipid levels, and that LINE-1 methylation was often seen in type 2 diabetes mellitus. In contrast to cancer, LINE-1 hypomethylation was associated with a higher risk of metabolic status worsening (Xiao-Jie, L., et. al. 2016). LINE-1 methylation was in general found more often in patients with higher LDL cholesterol and decreased HDL cholesterol levels, both favoring cardiovascular diseases (Xiao-Jie, L., et. al. 2016). LINE-1 retrotransposition can also affect the immune system. Aberrant LINE-1 expression can lead to strong stimulation of the innate immune system, therefore leading to higher autoimmunity and inflammation (Xiao-Jie, L., et. al. 2016). Inhibition of active LINE-1 elements has become a well-known strategy for treating various diseases (Xiao-Jie, L., et. al. 2016). During embryogenesis LINE-1s are normally active in the germline and get epigenetically suppressed in somatic cells. Interestingly in hypomethylated states, for example in many tumors, LINE-1s tend to get reactivated in somatic cells as well as during cancer initiation and progression (Xiao-Jie, L., et. al. 2016). Finding new ways to compensate the missing LINE-1 regulation upon hypomethylation in different cancer types becomes more important for the organism. Without proper control, LINE-1 elements, especially in cancer cells that are already characterized by enriched mutations, can lead to an even higher occurrence of mutations and to poor clinical outcomes (**Figure 6**).

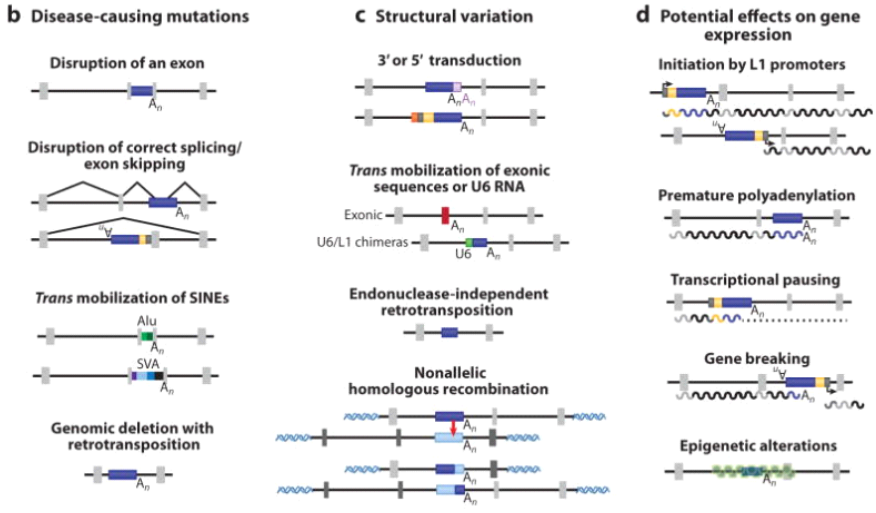

Figure 6 | Consequences of LINE-1-mediated retrotransposition events in humans.
LINE-1 insertion can lead to disease-causing mutations. Its actions can lead to exon disruption, disruption of correct splicing sites or exon skipping, by trans-mobilization of SINEs and through genomic deletions. LINE-1 TEs can also influence the structural variation of genes by transduction, homologous recombination and many more processes. LINE-1 insertions affect gene expression in a variety of ways, its adenosine-rich nature can for example induce unwanted polyadenylation as well as the introduction of

RNA polymerase II transcriptional pause sites on genes *(Beck, C. R., Garcia-Perez, J. L. et. al. 2011)*. Figure taken from *Beck, C. R., Garcia-Perez, J. L. et al. 2011.*

LINE-1 Transposase containing Domain 1 (L1TD1) as a LINE-1 derived domesticated gene is suspected to be such a potential LINE-1 regulator *(McLaughlin, R. N. et al. 2014)*. Its structural similarity and especially its RRM (RNA-Recognition-Motif), which originated from the ORF1 of LINE-1 (**Figure 7**), suggests that L1TD1 has the ability to recognize and bind LINE-1 RNA. How and under which conditions the proposed L1TD1 regulation functions remains to be unknown. To further understand the interplay between those two closely related genomic elements (LINE-1 and L1TD1), the general function of L1TD1 has to be understood and further studied.

1.7. L1TD1

Many of the domesticated genes directly originated from retroviral integration, while there is only one known example for a LINE-1 derived domesticated gene, the L1TD1 gene. L1TD1 has nearly all its protein-coding regions from its ancestor LINE-1 *(McLaughlin, R. N. et al. 2014)*. The origin of L1TD1 out of a specific LINE-1 gene element is shown in **Figure 7**.

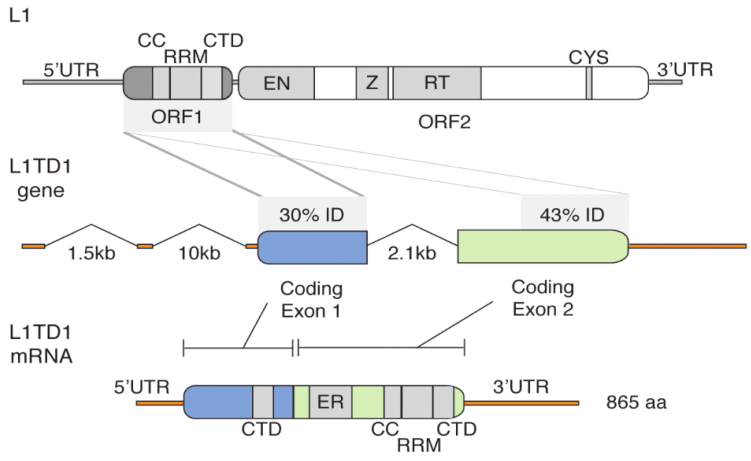

Figure 7 | The origin of L1TD1. L1TD1 originated from the ORF1 of the LINE-1 gene element. This could have happened through independent insertions or duplication events after a single insertion of ORF1. Within the L1TD1 gene these two elements are part of coding exons 1 and 2, sharing 30% and 43% amino acid identity respectively to their ancestor gene ORF1. Coding exon 1 encodes only the C-terminal-domain (CTD) and coding exon 2 the coiled-coiled (CC), RNA-recognition-motif (RRM) and the C-terminal-domain (CTD) of ORF1. After splicing events, L1TD1 mRNA makes up 3849 nucleotides and

encodes an 865 amino acid protein (*McLaughlin, R. et. al. 2014).* Figure taken from *McLaughlin, R. N., Young, J. M., et al. 2014*.

L1TD1 has lost the reverse transcriptase activity from its ancestor LINE-1, making it unable to change location within the genome (*McLaughlin, R. N. et al. 2014*). L1TD1 was lost or even pseudogenized multiple times during the mammalian evolution but returned with a more recent L1 ORF1 from the prosimian genome, suggesting its potential importance for the organism. It is known that L1TD1 evolved under positive selection in primate and mice, probably to function as a defense system against other retroviral elements, like LINE-1 (*McLaughlin, R. N. et al. 2014*). Interestingly, L1TD1 shows a very limited expression across adult tissues in humans (*Tissue expression of L1TD1 - Summary. (n.d.). The Human Protein Atlas*). It is only higher expressed in cells of the placenta, testis, cerebellum, colon and appendix (**Figure 8**).

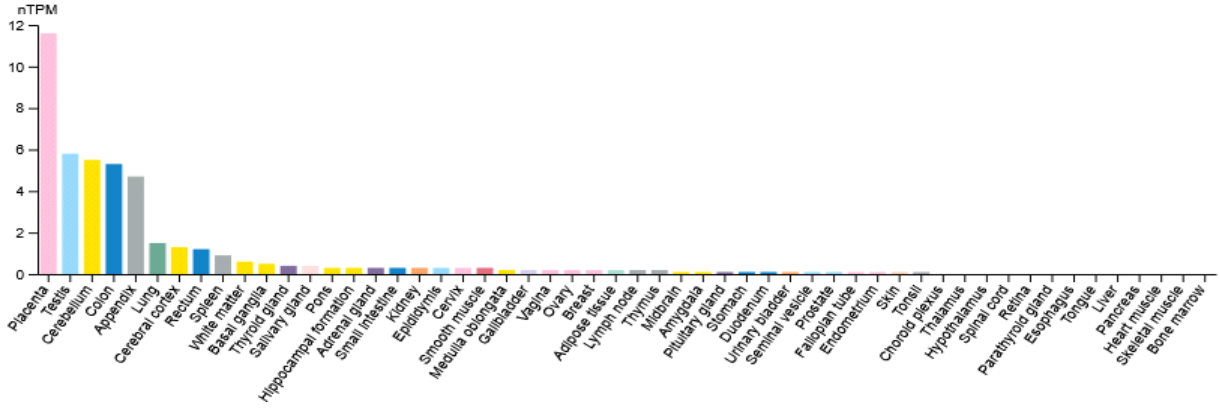

Figure 8 | L1TD1 RNA expression in different human tissues. High L1TD1 expression is only found in a few human organs. Figure taken from *Tissue expression of L1TD1 - Summary. (n.d.). The Human Protein Atlas.*

L1TD1 was originally identified as pluripotency marker in murine and human embryonic stem cells (ESCs) (*Wong, R. C. et al. 2011; Iwabuchi, K.A. et al. 2011*). L1TD1 was reported to be required for maintenance of pluripotency in human ESCs (*Närvä, E. et al. 2012*), while L1TD1 knockout (KO) in the mouse had no obvious phenotype (*Iwabuchi, K.A. et al. 2011*).

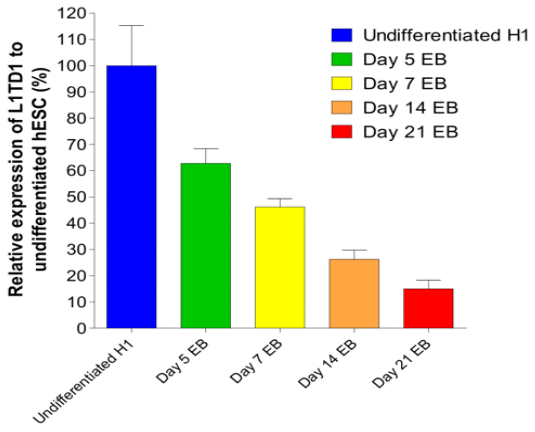

Figure 9 | mRNA expression of L1TD1 in undifferentiated and differentiated human ESCs. The graph nicely depicts the decreased L1TD1 expression upon increased cellular differentiation. Figure taken from *Wong, R. C. et al. 2011.*

In this context, Nanog, an important transcription factor involved in the self-renewal of stem cells, was identified to interact with the upstream promoter region of L1TD1, thereby activating its expression *(Wong, R. C. B. et al. 2011)*. The depletion of L1TD1 resulted in immediate downregulation of OCT4 and NANOG, reinforcing its role in the self-renewal and differentiation process of human ESCs (*Närvä, E. et al. 2012*). The L1TD1 interactome revealed its potential involvement in RNA splicing, translation, protein traffic, and degradation as well as its interaction with many stem-cell specific proteins *(Emani, M. R. et al. 2015)*. L1TD1 was also described as a new prognostic marker for early stages of colon cancer, where increased expression was associated with longer survival rates *(Chakroborty, D. et al. 2019)*. In contrast to these studies, seminomas, testicular germ cell tumors and medulloblastomas show high L1TD1 expression levels that are seen as beneficial for the cancer cells survival *(Närvä, E., Rahkonen, N., et. al. 2012).* Downregulation of L1TD1 led to less proliferation, reduced viability, higher apoptosis rates and more sensibilization of the tumor towards chemotherapeutic drugs. Most of these tumors came from pluripotent germ cells, which already had high L1TD1 expression levels *(Santos, M. C. T., Silva, P. B. G., et. al. 2015).* Despite the existing differences of L1TD1 levels in various cancer cell lines, its importance in the tumor cell can hardly be denied.

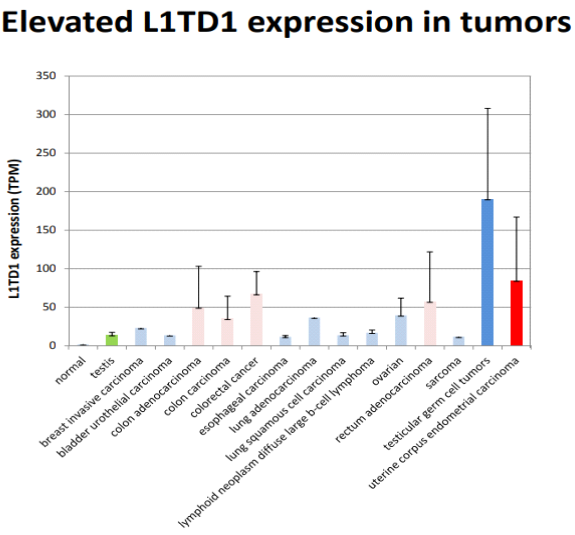

Figure 10 | L1TD1 RNA expression levels, analyzed in 11670 human samples. Compared to normal tissues, L1TD1 shows an increased expression in specific tumor variants, especially seen in testicular germ cell tumors. Figure taken from *Tissue expression of L1TD1 - Summary. (n.d.). The Human Protein Atlas*.

A frequent down-regulation of L1TD1 mRNA expression in primary tumors, colon, gastric and breast cancers was observed (**Figure 11**) (*Sun, Z. et al. 2022*), *Chiu, C. C et al. 2017, Altenberger, C. et al. 2017*). In contrast to L1TD1, LINE-1 RNA expression seemed to be upregulated in different cancer samples (*Altenberger, C. et al. 2017*). Studies on L1TD1 even showed that upon L1TD1 KO a decrease of LINE-1 promoter methylation resulted, which thereby led to higher LINE-1 activity. It is suspected that L1TD1 could have originally evolved for the genome defense against LINE-1 (*McLaughlin, R. N. et al. 2014).*

LINE-1 is known to provide the machinery for transposition of non-autonomous elements, which might also be the interaction platform with L1TD1. Moreover, L1TD1 could also function as a LINE-1 restriction factor, through interfering with the homodimerization of the LINE-1-ORF1 protein. On the other hand, there is also the theory that L1TD1 might outcompete L1 ORF1p for the binding to ORF2p (*McLaughlin, R. et al. 2014),* or that it inhibits the LINE-1 activity more upstream by influencing its methylation status (*Chiu, C. C et al. 2017)*. Furthermore, L1TD1 could also just bind to the RNA of LINE-1, thereby minimizing its spreading (*McLaughlin, R. et al. 2014).*

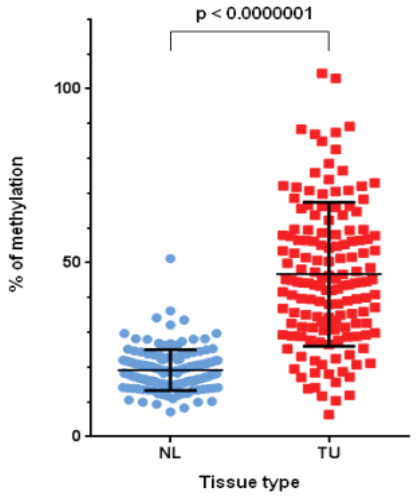

Figure 11 | Tumor specific L1TD1 methylation determined by MS - HRM (Methylation-Sensitive High Resolution Melting) analysis. L1TD1 shows low methylation status in non-malignant lung tissue but a significant methylation enrichment for primary tumor sample (TU). Figure taken from *Altenberger, C. et al. 2017*.

The L1TD1 interactome in human embryonic stem cells furthermore shows many important interaction/binding partners (**Figure 12**) (*Emani, M. R., et al. 2015*). L1TD1 interacts with U2af1 and Srsf3, which plays an important role in the reprogramming of somatic cells. It is also present in an interaction network with the human ESC marker panel of OCT4, SOX2 and NANOG, bridging nuclear and cytoplasmic regulation (*Emani, M. R., et al. 2015*).

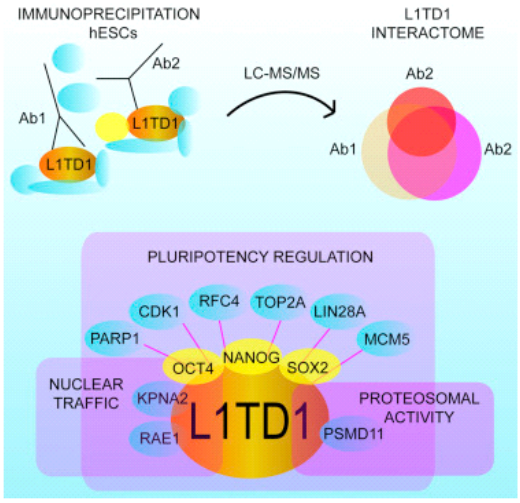

Figure 12 | Schematic of an L1TD1 Immunoprecipitation and its associated proteins. After successful immunoprecipitation a huge network of L1TD1 interaction partners was identified in human ESCs with protein sets involved nuclear traffic or proteasome activity (*Emani, M. R., et al. 2015)*. The largest proportion of the interactome consisted of proteins playing a role in the pluripotency regulation and thereby being linked to OCT4, SOX2 and NANOG. Figure taken from *Emani, M. R., et al. 2015.*

Gathered data about L1TD1 conclude that it might play a role in pluripotency regulation, in RNA splicing, in translation, in protein traffic and degradation processes in mammalian cells. However, deeper mechanistic insights into the cellular function of L1TD1 as RNA-binding factor are still missing.

2. Materials and Methods

2.1. In vitro work with human cells

For this study OV-90, an epithelial-like cell line isolated from the lung of a female patient with malignant papillary serous adenocarcinoma (*Cellosaurus cell line OV-90 (CVCL_3768). n.d.*), and HAP-1, a human near-haploid cell line which derived from a chronic myelogenous leukemia cell line (*OLS Ontology Research EMBL-EBI. n.d.)* were used.

Name of the cell line	Features/Genotype
OV-90 WT	Ovarian cancer - wildtype cell line
3B-KI	OV-90 cell line expressing C-terminal V5-tagged L1TD1
15B	OV-90 cell line with low L1TD1 expression
HAP-1 WT	human near-haploid cell line
KO	HAP-1 cell line with DNMT1 knockout
dKO	HAP-1 cell line with DNMT1 and L1TD1 double knockout
V5-KI	HAP-1 cell line expressing C-terminal V5-tagged L1TD1
1D	HAP-1 cell line expressing C-terminal V5-tagged L1TD1 subclone derived from V5-KI

For HAP-1 cells IMDM Medium (*Iscove's Modified Dulbecco's Medium – Sigma Aldrich*) was used.

Supplemented with:

10% Fetal Bovine Serum (FBS)

1% L-Glutamine

1% Penicillin/Streptomycin

Temperature: 37°C

Atmosphere: 95%, Air: 5% CO_2

For OV-90 cells, the base medium was a 1:1 mixture of MCDB 105 medium (*Sigma Aldrich*) and Medium 199 (*Gibco™ 11825015*) (filtered). For the complete growth medium the following supplements were added:

15% Fetal Bovine Serum (FBS)
1% Penicillin/Streptomycin

Temperature: 37°C
Atmosphere: 95%, Air: 5% CO_2

2.1.1. Cell thawing

Cells were rapidly thawed in a water bath (37 °C). Then the cells were pipetted into 15 ml tubes with 5 ml of pre-warmed media in it and centrifuged at 0.4 rcf for 3 minutes at RT. Subsequently, the supernatant was discarded, the cell pellet was resuspended in an appropriate amount of medium and transferred to a cell culture petri-dish.

2.1.2. Cell passaging

When cells reached around 70 - 90 % confluency, they were split or expanded to a larger surface in order to sustain their normal growth. The old media was aspirated, and the cells were washed 3x with 1xPBS. For cell detachment 1x trypsin-EDTA (*Gibco® Life Technologies*) was used. HAP-1 cells were incubated for 5 min at 37°C with trypsin, while OV-90 cells needed up to 10 min incubation for proper detachment. Gentle tapping of the flask or pipetting the Trypsin-EDTA solution on the cells helped. Subsequently Trypsin-EDTA was diluted with medium (1:2). The cells were then transferred into 15 ml sterile tubes and centrifuged at 0.4 rcf for 3 minutes at RT. The supernatant was removed, and the cell pellet resuspended in an appropriate volume of medium and transferred on new plates or cell culture flasks.

2.1.3. Cell counting

For estimation of cell numbers per plate, as well as for precise cell seeding and freezing, cells were counted by using a 4 % Trypan blue solution (*Thermo Fisher Scientific*) and the Countess® Automated Cell Counter (*Thermo Fisher Scientific*). The cell suspension was mixed with 0.4 % Trypan blue solution in a 1:1 ratio and 20 µl were pipetted into a Countess™ Cell Counting Chamber Slide (*Invitrogen*). This device also showed the number of viable cells.

2.1.4. Cell freezing

Cells were trypsinized and centrifuged (*see 2.1.2. Cell passaging*). HAP-1 cells were resuspended in 500 µl FBS with 10% DMSO (*Sigma-Aldrich*) and OV-90 cell lines in 5% DMSO (*Sigma-Aldrich*). Due to the cytotoxicity of the DMSO cells were rapidly aliquoted into 1.5 ml cryovials and stored at -80 °C or -120°C, for longer times.

2.1.5. Transfection of HAP1/OV90 cells

One day before transfection around $2x10^5$ cells were transferred in a 6-well plate and grown to 70% confluency. Cells were transfected with Lipofectamine transfection reagent (*GIBCO BRL*). Each transfection consisted of 1 ml reduced serum media (*Opti-MEM™, Life Technologies*) containing 1 µg of DNA and 7-12 µl of Lipofectamine reagent. Lipofectamine and the DNA were separately mixed with 0.5 ml of reduced serum and incubated for 15 min at RT. The Lipofectamine mix was then slowly pipetted to the DNA mix and again incubated for 20 min at RT. The transfection mix was subsequently dropwise added to the cells. Later, 5hrs after transfection 1 ml of IMDM with 15% FBS was added. In order to check transfection efficiency under these conditions a GFP plasmid was used as control and after 24 hours the cells were checked using an inverted microscope with fluorescent mode. About 10-20% cells gave positive GFP signals.

2.1.6. Limited Dilutions

When the cells were dense enough, the medium was removed, and the cells were washed 2x with 1 ml 1xPBS. Then the cells were trypsinized (200µl, 1x Trypsin-EDTA, *Gibco® Life Technologies*, see chapter *2.1.2. Cell passaging*) and put in the incubator for 5 min at 37°C. After incubation 2 ml of the appropriate medium was added. Subsequently cells were

resuspended and counted, see chapter 2.1.3. *Cell counting.* Then the cell concentration was adjusted to $3x10^5$ cells/ml (for 2x348-well plates). For the next step 3x 1:10 serial dilutions were made (100µl cells + 900µl media). For the last dilution, the cells were diluted 1:20 in 50 ml falcon tubes (38ml medium) to get a final concentration of 15 cells/ml. 50 µl of the last mix was transferred in two 384-well plates. Then we had to wait for approximately 2-4 weeks for the clones to grow. A backup of cells was frozen away from a 6-well plate, see chapter *2.1.4. Cell freezing.*

2.1.7. Clone picking

2-4 weeks after performing the limited dilutions, clones were picked. Large single colonies were identified under the light microscope and then softly scraped off with the tip of a pipette and transferred to a 96-well plate. This process was repeated several times until the cell density and number was enough for other experiments. Later, when the cell density was higher, cells were not scraped anymore but trypsinized for expansion, see chapter *2.1.2. Cell passaging.*

2.2. Work with proteins

2.2.1. Harvesting cells for protein extraction

Cell plates were washed 3x with pre-cooled 1xPBS. Then they were scraped off with 5 ml of 1xPBS on them and transferred into a sterile 15 ml tube. The tubes were centrifuged for 5 minutes at 450 rcf at 4 °C. The supernatant was discarded, and the pellet was resuspended in 1 ml of 1x PBS and transferred to a 1 ml Eppendorf tube. The cells were again centrifuged with a small desk centrifuge for 5 minutes at 450 rcf on 4°C. Then the supernatant was carefully removed, and the pellet quickly shock frozen in liquid nitrogen. Short time storage took place in a -80°C freezer, while for the long term storage a -120°C liquid nitrogen freezers was used.

2.2.2. Protein isolation

Proteins were isolated using the freeze and thaw method. Hunt buffer supplemented with fresh protease inhibitors was used for cell lysis. The frozen cell pellet was thawed on ice and resuspended in an appropriate volume of Hunt buffer (30µl-150µl). For cell lysis, the cells were

snap frozen in liquid nitrogen and thawed (37 °C), this process was repeated three times followed by centrifugation for 30 minutes at 13.523 rcf at 4 °C. The supernatant was transferred to a new sterile 1 ml tube and the protein concentration was measured, see *Bradford assay 2.2.3.* After protein measurement the supernatant was frozen at -20°C or for longer storage at -80°C.

Hunt buffer

20 mM Tris/HCl (pH 8.0)
100 mM NaCl
1 mM EDTA
pH adjusted to 8.0

Proteinase/Phosphatase Inhibitors

0.5 % NP-40 Protease inhibitors were added before use.
Protease inhibitors
50x PI (cOmplete protease inhibitor cocktail tablet; 1 tablet dissolved in 1 ml dH2O; Roche) 100x β-glycerophosphate disodium hydrate
100x sodium fluoride 200x aprotinin
1000x sodium molybdate
1000x sodium orthovanadate (prior to use activated at 95 °C for 5 minutes)
1000x PMSF (phenylmethane sulfonyl fluoride)

2.2.3. Bradford assay

Bradford protein assay was used to measure the total protein concentration in a solution. Protein Assay Dye Reagent Concentrate (*Biorad*) was diluted in a 1:5 ratio with dH_2O and mixed with 1 µl sample in 1 ml tubes. The absorption was measured against the blank value (1 µl Hunt buffer) with NanoDrop™ One C (*Thermo Fisher Scientific*) at 595 nm by using cuvettes. Absorption values were multiplied with 10 to obtain concentrations in µg/µl.

2.2.4. Sodium dodecyl sulfate-polyacrylamide gel electrophoresis (SDS-PAGE)

This method was used in order to separate the isolated proteins according to their molecular weight. Depending on the protein size, the concentration of acrylamide (density of the gel) was adapted. The separation gel had a range from 10-15% and for the stacking gel we always stuck to 5%.

20 µg of protein was used and 5 x SDS loading dye was added to the sample. Then the samples were heated for 5 minutes at 95°C, which led to the disruption of the secondary and tertiary structures of the proteins. The SDS is important for the following separation process, since it overlays the charge of the proteins and gives them a constant negative charge. Due to the denaturation and the electrostatic repulsion of the negative charges, the proteins were linearized and migrated through the gel in the direction of the positive pole. The proteins were separated using 15-20 mA. When samples reached the separation gel, the amperage was increased to 30 mA. In order to follow the protein migration, 4 µL of Precision Plus Protein Ladder (*ThermoFisher*) was used. The gel ran in a 1x Running Buffer.

Separation Gel	10% (2 gels)	Stacking Gel	5% (2 gels)
30% acrylamide	4 ml	30% acrylamide	510 µL
1M Tris-HCl (pH 8.8)	3.75 ml	1M Tris-HCl (pH 6.8)	375 µL
dH2O	4.15 ml	dH2O	2.1 µL
20% SDS	60 µL	20% SDS	15 µL
20% APS	65 µL	20% APS	28 µL
TEMED	7.5 µL	TEMED	7.5 µL

30% Acrylamide (*BioRad*)

Separation Buffer
375 mM Tris/HCl
0.1% SDS
diluted in dH_2O
pH adjusted to 8.8 using HCl
Stacking Buffer
125 mM Tris-acetat
0.1% SDS diluted in dH_2O
pH adjusted to 6.8
Ammonium persulfate (APS)
20% APS 58
diluted in dH_2O

Sodium-dodecyl sulfate (SDS)
20% SDS diluted in dH2O
SDS loading dye
100 mM Tris/HCl pH 6.8
20% Glycerol
0.01% Bromophenol blue
10% β-mercaptoethanol
5% SDS diluted in dH_2O
10x Running Buffer
14.4% Glycine
3% Tris/HCl
1% SDS diluted in dH_2O
pH adjusted to 8.3

2.2.5 Western Blotting

After the proteins were separated properly, the wet blot transfer was performed. For this the gel was gently removed from the glass plates, placed in a nitrocellulose membrane (*Whatman*) and was flanked by 3 mm filter papers, one on each side. The membrane and the filter papers were humidified before with the wet blot transfer buffer. On each side of the transfer cassette one wet sponge was placed. Before usage the wet blot chamber was filled up with the transfer buffer. The proteins will migrate from the gel to the membrane (from cathode to anode) and thereby will be transferred to the membrane, **Figure 13**.

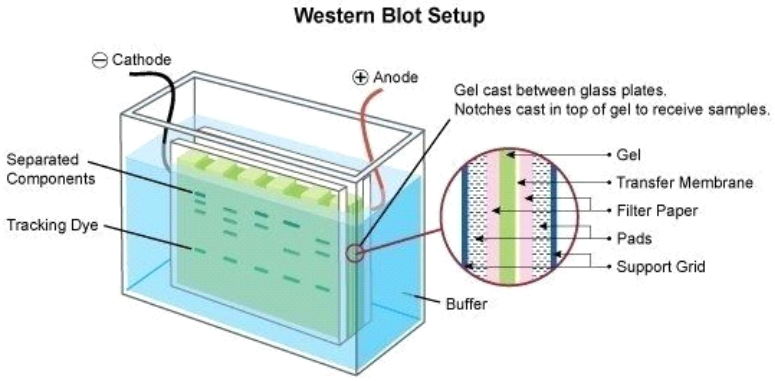

Figure 13 | Scheme of the Western Blot sandwich.
The by size separated proteins are migrating from the gel into the membrane, from the cathode to the anode. Picture taken from Holschbach, M. (n.d.). Western Blot: Gelelektrophorese für Proteine.

The transfer was performed using an amperage of 250 mA for 2 hours or 50 mA overnight at a temperature of 4°C. After the transfer, the membrane was stained for 2 minutes on a shaker using a 1x Ponceau staining solution. Then the Ponceau solution was gently washed off with dH_2O. To prevent the unspecific binding of the antibodies, the membrane was blocked with a Blocking solution for 30 minutes at RT on the shaker. After this, the membrane was incubated overnight at 4°C or for 3 hrs on RT on a tube roller together with the first antibody. The primary antibody was diluted in a 1x Blocking solution. After the incubation, the membrane was washed 3x for 5 minutes with 1x PBS-Tween (1x PBS containing 0.1% Tween-20) and was subsequently incubated with the second HRP-coupled antibody for 1 hour at RT. Then the membrane was washed again 3x for 5 minutes with 1x PBST and was ready to be used for protein detection.

Western Blot - primary antibody list:

Antibody	Animal	Clonality	Source (catalog or lot nr.)	Dilution
L1TD1	Rabbit	Polyclonal	sigmaaldrich (HPA280501)	1 : 1000
L1TD1	Mouse	Monoclonal	R&D (MAB8317)	1 : 25
LINE-1 orfp-1	Mouse	Monoclonal	sigmaaldrich (MABC1152)	1 : 1000
V5	Mouse	Monoclonal	MBL (M215-3)	1 : 1000
V5	Mouse	Monoclonal	sigmaladrich (V8012-50UG)	1 : 500
HDAC2 3F3	Mouse	Polyclonal	Seiser lab	1 : 1000
HDAC1 Sat 208	Rabbit	Polyclonal	Seiser lab	1 : 10000
DNMT1	Rabbit	Polyclonal	sigmaaldrich (D4692)	1 : 500
YY2	Rabbit	Polyclonal	abclonal (A16621)	1 : 1000
beta-actin	Mouse	Monoclonal	sigmaaldrich (A5316)	1 : 1000
beta-actin	Mouse	Monoclonal	Abcam (ab8226)	1 : 5000
Vinculin	Mouse	Monoclonal	Santa Cruz (sc-25336)	1 : 1000

Western Blot - secondary antibody list:

Antibody	Animal	Clonality	Source (catalog or lot nr.)	Dilution
Anti-mouse	Goat	Polyclonal	Jackson Laboratories	1:10.000
Anti-rabbit	Goat	Polyclonal	Jackson Laboratories	1:10.000
Anti-rat	Goat	Polyclonal	Cell signaling technology	1:10.000
Anti-goat	Donkey	Polyclonal	Jackson Laboratories	1:10.000

2.2.6. Immunodetection by enhanced chemiluminescence

In order to detect specific proteins *via* the bound primary and secondary HRP-antibody, the membrane was incubated for approximately 1 minute with super/ECL Western Blot detection reagents (*Solution A: Luminol/Enhancer, Solution B: Peroxide Buffer; GE Healthcare*) in a 1:1 ratio and subsequently visualized using the chemiluminescence imaging system (*Fusion FX, Vilber Lourmat*).

Wet transfer Buffer

3.024 g/L Tris/HCl pH 8.0

14.42 g/L Glycine

20% Methanol diluted in dH2O

pH adjusted to 8.0

10x Ponceau stain solution

2% Ponceau S

30% Trichloroacetic acid

30% Sulfosalicylic acid diluted in dH_2O

Blocking Solution

1% Milk powder

1% Polyvinylpyrrolidone

0.1% Tween-20

0.02% Sodium azide

10% 10x PBS diluted in dH_2O

pH adjusted to 7.4

1x PBS-Tween

10x PBS diluted in dH_2O

0.1% Tween-20

pH adjusted to 7.4

2.2.7. Western blot membrane stripping

To remove signals from previously added antibodies, Western blot stripping was performed.

With this method the primary and secondary antibodies from the membrane can be partially removed and therefore give less background signal. First the membrane was fully covered with the Stripping buffer and incubated on the shaker for 5-10 minutes at RT. Then the buffer was discarded and the procedure was repeated. After this the membrane was washed 2x 10 min with 1xPBS and 2x 5 min with 1xTBST (PBS-Triton (1x PBS/0.1 % Triton X-100)). In the end the membrane was blocked with Blocking solution for half an hour and was ready for the next antibody incubation.

Stripping buffer

25 mM glycine-HCl

1% SDS

0.01% Tween

fill up to 1 L deionized water

pH adjusted to 2.2

10X TBST Tris buffered saline

200 mM Tris-base

1500 mM NaCl

fill up to 1 L deionized water

pH adjusted to 7.6

2.2.8. Silver staining

Silver staining is used as a quick and sensitive method for protein detection. First the proteins are fixed, then they get sensitized and in the end a selective reduction of silver ions into metallic silver happens in close proximity to proteins (*Kumar G. at al. 2018*). The stain can easily be seen by eye and documented (Rice, D., & Galbraith, M. 2008).

After electrophoresis, the gel was placed in a tray, covered with 100 ml Fixation solution and shaken for 30 min on RT. The Fixation solution 1 was replaced by the Fixation solution 2 and shaken for an additional 20 minutes. Subsequently the gel was washed 3x 5 min with H2O.

Afterwards the H2O was decanted and around 98 ml of Protein sensitizer solution was added and shaken for 2 min. Then the gel was again washed 3x 1 min with H2O. For the staining the Protein staining solution was added for 15 min on a shaker. The stain was decanted, and the gel washed 3x 1 min with H2O. Then the Protein development solution was added and the tray with the gel was gently shaken while observing the stain development. Depending on the amount of protein loaded, the stain development happened faster or slower. Once the protein bands appeared, the solution got decanted and the Stop solution was added. This step needed to be fast, otherwise the bands can turn very dark. The gel can be stored dry or at 4°C covered with fresh Stop solution.

Silver staining Solutions:

Fixation Solution 1

50% methanol (or ethanol) v/v in H2O

0.05% formaldehyde

Fixation Solution 2

25% methanol (or ethanol) v/v in H2O

0.05% formaldehyde

Protein staining Solution (freshly prepared)

0.2% Silver Nitrate solution (w/v; 100 ml in H2O)

0.076% formaldehyde

Protein Sensitizer Solution (freshly prepared)

0.02% Sod. Thiosulfate w/v; 100 ml in H2O

Dilute 1:100 from a 2% stock solution

Developing Solution (freshly prepared)

6% sodium carbonate in 100 ml H2O

Stop Solution

10% methanol (or ethanol)

5% Acetic acid v/v in H2O

2.2.9. Immunofluorescence labelling of cells grown on coverslips

Indirect immunofluorescence analysis was used for the detection of a wide range of antibody bound proteins. The medium of the cells was aspirated from the wells, and the cells were washed once with ice cold 1x PBS. Afterwards the cells were incubated with 4 % paraformaldehyde (PFA) for 20 minutes at 4 °C under the hood. Then the PFA was disposed, and the cells were again washed twice with 1x PBS. For longer storage 1x PBS was added onto the cells, the plates were sealed with Parafilm and stored at 4°C. In order to block nonspecific epitopes, 4% goat serum in 1xPBS-Triton (1x PBS/0.1% Triton X-100) was prepared and added to the cells for 15 minutes. Subsequently, the mix of primary antibodies, together with 1xPBS-Triton in 4% goat serum was added and incubated overnight at 4°C on a rocking shaker. The following day the cells were washed 3x 10 minutes with 1x PBS-Tween (1x PBS containing 0.1% Tween-20) and the secondary antibody in 1x PBS-Tween and 4% goat serum was added. Incubation took at least 1 hour at RT in the dark. Afterwards the cells were washed again 3x 10 minutes with 1x PBS-Tween. Then DAP was added (1:1000 1x PBS) to the cells and incubated for 10 minutes on the shaker. For the last two washes 1x PBS was used and the coverslips with the cells were fixated on the microscope-coverslips with ProLong™ Gold (*ThermoFisher*) and dried in the dark. The Immunofluorescence-labeled cells were visualized and photographed using the Olympus CKX53 inverted microscope or the VS120 virtual slide systems (*Olympus BX61SV*) and Olympus VS-ASV software.

Immunofluorescence - primary antibody list:

Antibody	Animal	Source (catalog or lot nr.)	Dilutions
L1TD1	Rabbit	sigmaaldrich (HPA280501)	1 : 1000
L1TD1	Mouse	R&D (MAB8317)	1 : 25
LINE-1 orf1p	Rabitt	abcam (ab245249)	1 : 100
V5	Mouse	MBL (M215-3)	1 : 50
V5	Mouse	sigmaladrich (V8012-50UG)	1 : 50

Immunofluorescence – secondary antibody list:

Antibody	Animal	Source (catalog or lot nr.)	Dilutions
Alexa Fluor 546	Mouse	Invitrogen (A110003)	1 : 500
Alexa Fluor 488	Rabbit	Invitrogen (A32731)	1 : 500

2.2.10. Immunoprecipitation (IP) experiments

In order to gather information about possible protein-protein interactions IP experiments were performed. The principle of this experiment is the binding of specific antibodies to the protein of interest that can be pulled out of the cell lysate using magnetic beads. With this method also proteins that are interacting with the target protein can be isolated.
For this purpose, 500 µg of protein extract was used. Antibodies were prepared (6µg) and added to the protein suspension. The mixture was incubated O/N on a tube roller, 20rpm on 4°C. On the next day, 40 µl G-beads (*ThermoFisher*) were washed 3x with Hunt buffer. The protein-antibody extract was added to the beads, filled up to 300 µl with Hunt buffer and incubated together for 1-2hrs on a tube roller, 20rpm at 4°C. On the next day the beads were washed 2 x 5 minutes on the tube roller at 4°C with 1x TBS. The last wash with 1 x TBS took 15 minutes and was performed at 4 °C. For loading the precipitated proteins on the gel, the supernatant was discarded and the proteins sticking to the magnet beads on the magnetic rack were diluted with 40 µl SDS loading buffer and incubated at 95°C for 5 minutes. Then 20 µl of the protein samples were loaded on an SDS-gel.

10x TBS
200 mM Tris/HCl
1500 mM NaCl
fill up to 1 L deionized water
pH adjusted to 7.6

2.2.11. RNA-Immunoprecipitation (RIP)

RNA-immunoprecipitation (RIP) assays work very similar to the previously described IP. The only difference between them is that an RIP precipitates RNA too and gives insights into the RNA interactome as well as insights into the expression status of the protein of interest. The cell pellet was thawed on ice and the Polysomal buffer (PLB) with freshly added protease inhibitors was prepared. Around 500-800 µl of the buffer was added to the freshly thawed cell pellet dependent on the individual pellet size. Cell lysis was promoted using a 27g syringe to shear the DNA (about 20x times). Then the suspension was centrifuged at 13.523 rcf for 15 minutes at

4°C. The supernatant containing the RNA protein complexes was taken and and the protein concentration was measured using the Bradford assay, see section *2.2.3. Bradford assay*. For the RIP, 500-700µg of protein was needed and 20 µg was used as input for the Western blot analysis. Eppendorf tubes for the Western blot Input (20 µg), for the Protein IP (700 µg) and for the RNA Input (10%) were prepared.

The antibody was added to the protein suspension and incubated O/N on a tube roller 20 rpm at 4°C. On the next day vials for the G-beads (*ThermoFisher*) were prepared and 40 µl of the bead suspension were allotted per vial. The beads were washed 3x 5 minutes with PLB buffer containing 0.05U/µg RNAsin at 20 rpm on 4°C. Subsequently the beads were blocked with PLB buffer, containing 10% BSA (10mg/ml) for 30 minutes at 20 rpm at 4°C. The BSA solution got discarded afterwards and the protein-AB mixture was added to the blocked beads. Together they were incubated for 1-2 hrs. on 20 rpm at 4°C. After the incubation the supernatant was gathered and used as supernatant control sample together with the input sample for the following Western blot analysis. The amount of target protein remaining in the supernatant (unbound protein of interest) gave information about the efficiency of the IP. The beads with the protein-antibody complex were washed again 3x with 500 ml of PLB buffer. The first two washes were short - 5 minutes and the last wash took longer - up to 15 minutes. In the end 500 µl of PLB buffer was added and the samples were divided in a 1:5 ratio, one part was used to perform the Western blot analysis and one for the RNA analysis. Samples were stored at -20°C.

Western Blot:

Protein input from whole cell lysate

Protein supernatant after RIP

Immunoprecipitated Protein

Quantitative Real-Time PCR:

RNA input from whole cell lysate

RNA supernatant after RIP

Immunoprecipitated RNA bound to target protein.

PLB Buffer

100 mM KCl

5 mM $MgCl_2$

20 mM HEPES (pH 7.4)

0.5% NP-40

100 µg/ml Cycloheximide?

2mM DTT

40 U/ml RNase inhibitor

1x protease inhibitor cocktail

pH adjusted to 7.5

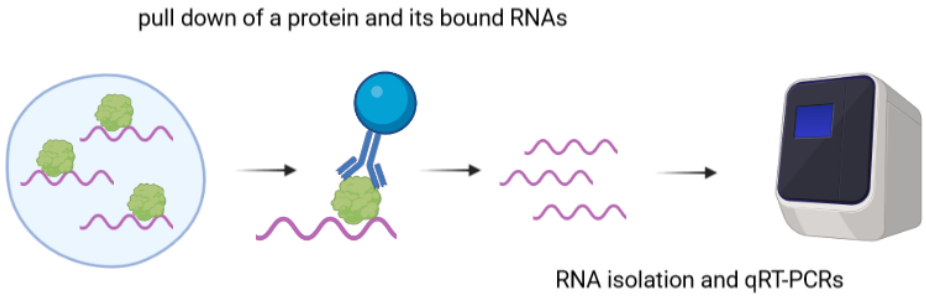

Figure 14 | Overview of the main RNA immunoprecipitation steps.
From cell lysis to protein and RNA extraction. Antibodies bind to the proteins which in turn are bound to RNA (in case of RIP). If the binding is strong enough, the antibodies, which are pulled down by the magnetic beads, will also pull down the protein-RNA complex. After the RNA isolation RT-qPCR can be performed. *Picture created with BioRender.com*.

For evaluation of the RNA-IP, the RNA was reverse transcribed to cDNA, see *section 2.6.2. Reverse transcription,* and then amplified using specific primers, see *section 2.6.3. Quantitative Real-Time PCR*. To check RNA quality, an RNA-MOPS gel was casted, see *section 2.6.1 RNA isolation*. The protein-IP was analyzed on a Western blot, see *section 2.2.5 Western Blotting*.

2.2.12 Mass spectrometry

Mass spectrometry was used to compare the proteomes of HAP-1 KO and dKO cells. Biological triplicates of 10 cm cell plates of HAP-1 KO and dKO cells were grown on 10 cm cell plates, the cell pellets were harvested, see *section, 2.2.1. Harvesting cells for protein extraction*, and snap frozen in liquid nitrogen. The frozen samples were then handed over to the Mass-spec facility at the Vienna Biocenter for mass spectrometry analysis.

2.3 Generation of OV-90 cell lines with a V5-tagged L1TD1 version or a knockout L1TD1 version using CRISPR/Cas9 technology

CRISPR/Cas9 is a powerful genetic engineering tool for efficient gene editing. An RNA-guided Cas9 nuclease that initially was found in the adaptive immune system of bacteria has the ability to precisely cut DNA. To find the target site, a so -called guide RNA can be specifically designed. This guide RNA will lead the nuclease to the right cutting sites. (Ran, F. *et al.* 2013). After the cutting different cellular repair mechanism can jump in, see (**Figure 15b**).

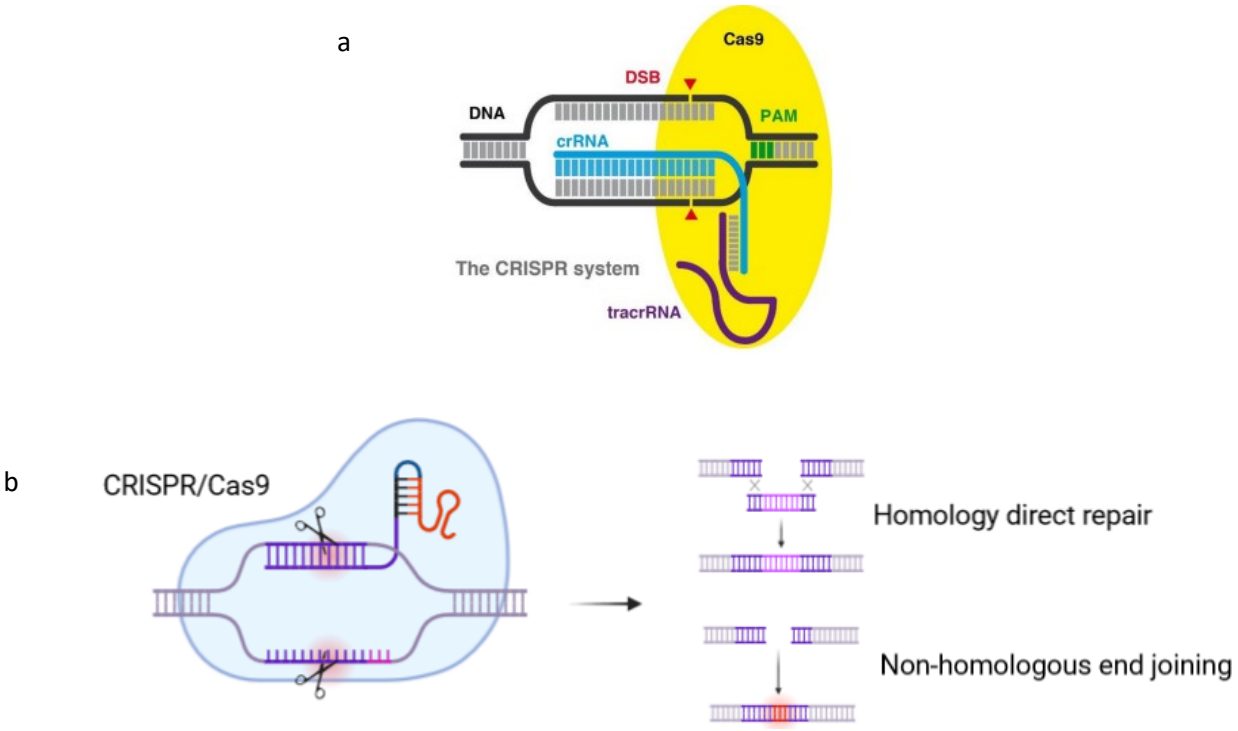

Figure 15 | Overview of the CRISPR/Cas9 method. a. For genome editing purposes a single guide RNA (sgRNA) was created by connecting the bacterial CRISPR RNA (crRNA) to the trans-activating crRNA (tracrRNA). Together they form a complex, called the sgRNA. The sgRNA can be specifically designed to target the region of interest that is present in the genome. Upon targeting the endonuclease Cas9, recognizes the PAM sequence located at the 3' end of the protospacer and induces a double strand break (DSB). **b.** Dependent on the repair mechanisms that is used, the CRISPR/Cas9 tool can induce knock-in and knock-out mutations as well as the introduction of point mutations, see *Figure 15b*. Figure 15a was taken from *Montoliu, L. et al. (n.d) The CRISPR web page, Figure 15b* was created with BioRender.com.

2.3.1. Electroporation of OV-90 cells

For electroporation as first step of L1TD1 gene editing OV-90 cells were grown on 10 cm plates. When the cells reached around 70 % confluency, they were used for electroporation.
First the complex formation of the tracerRNA and crRNA had to take place. For this 3.2 µl of the tracrRNA (320pmol) and 3.2 µl of the crRNA were mixed with 9.9 µl IDTE. Then the mixture was placed into a thermocycler in order to promote the guide-RNA complex formation. Afterwards the gRNA (16.3 µl, 12µg) was added to 1.5 µl of Cas9 protein (5 µg) and incubated for 5-10 minutes on RT.

PCR scheme of guide-RNA complex formation

Time (s)	**Cycles**
94°C	5min
93°C	20s -1°/cycle x 12 cycles
80°C	4min
79°C	20s -1°/cycle x 3 cycles
75°C	4min
74°C	20s -1°/cycle x 3 cycles
70°C	4min
69°C	20s -1°/cycle x 59 cycles
10°C	forever

IDTE Buffer
10 mM Tris/HCl
0.1 mm EDTA
pH: 7.5

In the meanwhile, cells were trypsinized and counted. For this experiment $1x10^6$ cells were used. After the cells were centrifuged at 0.4 rcf for 3 minutes at RT, the calculated amount was diluted in 1 ml of 1xPBS. This cell aliquot was again centrifuged and the supernatant was aspirated. The cells were now resuspended in 115 µl of R Buffer (Resuspension buffer, *Invitrogen*™) and Cas9. Then the sgRNA mixture was added and gently mixed together. In order to avoid bubbles a total volume of more than 100 µl is recommended when electroporating.
For the insertion reaction to take place, 2 µl of HDR (400 pmol; homologous DNA for insertion) was added to the cell lysate. For generation of a V5-tagged L1TD1 HDR harbored a hL1TD1-V5-

tag, which was kindly provided by Terezia Vcelkova. As control a GFP-Plasmid (2 µl of pX552-GFP), which again was kindly provided by Terezia Vcelkova was used. For the knockout reaction no HDR was added.

Afterwards the electroporation column was filled with 3 ml of E-Buffer (Electroporation buffer, *Invitrogen™*). The cells with and without the HDR-template, the Cas9 and the sgRNA were resuspended and loaded onto the Neon-tip of the electroporation machine (*Invitrogen™Neon™ Transfection System*). Conditions for the electroporation: 1575V, 10 wdhs, 3 pulses.

The sgRNA sequences used in this experiment:

target Gene	V5 KI sgRNA Sequence (5' – 3')	V5 KI Sequence (5' – 3')	Company
L1TD1	ttgagagaattactggggaat	ggtaagcctatccctaaccctctcctcctcggtctcgattctacg	horizon

target Gene	L1TD1 KO sgRNA Sequence (5' – 3')	Company
L1TD1	tgatgaaaggtcggctacca	horizon

2.3.2 Clonal dilution and expansion of cell lines

The electroporated cells were first transferred to 10 cm plates in order to regenerate from the stressful electroporation process. On the next day, the GFP control was checked under the fluorescence microscope. GFP positive cells indicated a successful electroporation/DNA insertion event. After an additional day of cultivation part of the electroporated cells were frozen away and the rest was used for serial dilutions.

The medium was removed, and the cells were washed once with 1x PBS. The cells were trypsinized and counted. Then 3x 1:10 serial dilutions were made, and from the last dilution the cells were again diluted in a 1:20 ratio (50 ml falcon). The goal was to reach a concentration of 15 cells/ml. Using a multichannel pipette, 50 µl of the final dilution was pipetted into each well of a 384-well plate. Since OV-90 cells were characterized by a very slow cell growth when isolated from their neighboring cells, we approximately waited 3-4 weeks to proceed with the clone picking. Wells with nice, observable single cell colonies were picked and expanded on 96-well plates by gently scraping the cells off with the tip of a pipette. The clones were stepwise expanded to 24-well, 12-well and 6-well plates (using trypsinization), until the cell amount was high enough for protein isolation. Cellular proteins were extracted and tested for the presence of the V5-tagged L1TD1 protein by Western blot analysis.

2.3.3 Validation of the knock-in and screening of cell clones (PCR, Western blot, IF)

As described in section *2.5.2 Clonal dilution and expansion of cell lines*, the electroporated cells were analyzed on Western blots (when they reached higher densities ~ 70%). The screening of clones was performed by running different PCRs (nested and screening/direct PCR). All these PCR assays were used to test if the transgene at the L1TD1 locus was present. The primers pair was either binding outside of the integrated transgene or within it.

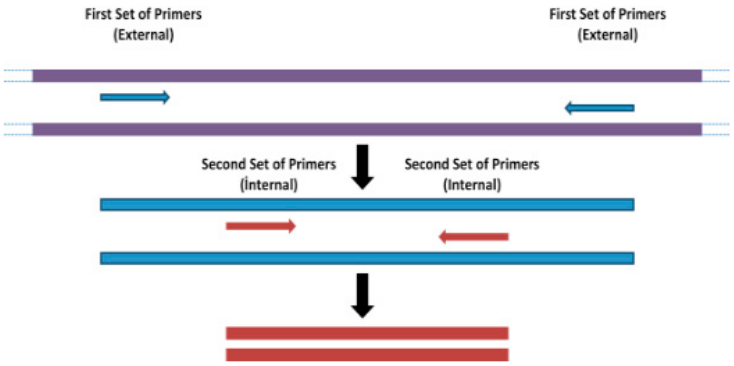

Figure 16 | Overview of a nested PCR Analysis. In the nested PCR two different sets of primers are used. In the first PCR round, primers that bind outside of the target sequence will amplify a bigger fragment. In the second PCR round the big fragment is used as a template for the next PCR that targets a smaller region within the first PCR product. Nested RT-PCR can increase the sensitivity and specificity of the reaction (Green, M. R., & Sambrook, J. 2019). Figure taken from *Green, M. R., & Sambrook, J. 2019.*

For our knock-in validation we used a direct PCR with a primer pair that targeted the right and left homology arm of L1TD1 and a nested PCR with an additional primer set binding within the L1TD1 gene.

2.4 Work with RNA

2.4.1 RNA isolation

For RNA isolation from cells/cell pellets the TRIzol® reagent (Life Technologies) was used. TRIzol reagent is a chemical that maintains the RNA integrity, while it disrupts the cells and dissolves other cell components. Before starting, all used surfaces and the equipment were cleaned with 1 M NaOH, in order to get rid of the omnipresent RNases. The RNA isolation procedure was carried out using a RNA isolation kit (*Monarch® Total RNA Miniprep Kit, NEW ENGLAND BioLabs).*

First, the medium from the plates was removed and the cells were washed with 1x PBS. Cell lysis took place by adding 1 ml TRIzol® reagent. Cells and the TRIzol solution were incubated for 1 minute at RT. The lysed cells were then immediately transferred to 1.5 ml sterile tubes and 200 µl of chloroform was added. The tube was vigorously vortexed for 15 seconds and centrifuged at 13.523 rcf for 15 minutes in a pre-cooled centrifuge at 4 °C.

For RNA precipitation, only the upper aqueous phase was used and was transferred to a new sterile 1.5 ml tube. Then 1x volume of EtOH (>95%) was added and was mixed by flicking the tube. The RNA cleanup column was inserted into a collection tube and the sample was loaded onto a column (all provided in the kit). The tube was centrifuged for 1 minute at 13.523 rcf at 4°C and the flow-through was discarded. Then the column was re-inserted into a new collection tube, 500 µl of RNA Cleanup Wash Buffer was added and centrifuged again under the same conditions. The flow-through was discarded, the column re-inserted into a new collection-tube and again 500 µl of RNA Cleanup Wash Buffer (provided in the kit) was added. After centrifugation under the same conditions the column was centrifuged for an additional minute to ensure that all traces of salt and EtOH disappear. For RNA elution 20 µl of nuclease-free water was added and centrifuged for 1 minute in a new sterile, 1.5 ml elution tube. The RNA concentration was measured using NanoDropTM One C (*Thermo Fisher Scientific*). In order to evaluate the quality and concentration of the isolated RNA, a MOPS gel run was carried out. For this 500 ng RNA samples were prepared and mixed with 2 µl EtBr-loading buffer (*Sigma Aldrich*). The mix was filled up with dH_2O to 10 µl and heated to 65 °C for 5 minutes in a thermomixer. Subsequently the RNA was loaded on a MOPS gel, which ran for 20 minutes at 90 V in a 1x MOPS buffer. Visualization followed, using the ChemiDoc XRS+ system (*Biorad*).

MOPS Gel

1.2 g agarose (*SeaKem® LE Agarose, Lonza*)
90 ml sterile dH2O
10 ml 10x MOPS buffer
5.2 ml formaldehyde (added after boiling the gel)

10x MOPS buffer

0.2 M MOPS
50 mM sodium acetate (pH 5.0)
10 mM EDTA
(diluted in dH_2O and adjusted to pH 7.0 with NaOH, kept at 4 °C)

RNA loading buffer

15 ml deionized formamide
4.8 ml 37 % formaldehyde
3 ml 10x MOPS
2 ml dH_2O
2 ml glycerol
1.6 ml 10 % bromophenol blue
5 µl EtBr
pH adjusted to 8.0

2.4.2. Reverse transcription

Via reverse transcription cDNA can be synthesized from isolated RNA. The enzyme reverse transcriptase (RT) enables this synthesis out of the complementary DNA (cDNA). For this reaction 500 ng of isolated RNA was mixed with 4 µl 5x iScript Reaction Mix and 1 µl iScript Reverse Transcriptase from the iScript cDNA Synthesis Kit (*Biorad*). The mix was filled up to 20 µl with nuclease-free water. The reaction was carried out in a thermocycler according to the following this scheme:

Temperature (°C)	Time (min)
25	5
46	20
95	1
4	∞

2.4.3. Quantitative Real-Time PCR

The cDNA from the reverse transcription was diluted in a 1:10 ratio with ultrapure dH2O.
Per reaction, 5 µl diluted cDNA, 10 µl Sso Advanced Universal SYBR Green Supermix (*Biorad*), 0.4 µl of 10 µM forward and reverse primer were mixed and filled up to 20 µl with sterile dH_2O. Each reaction was conducted in duplicates.
The primer annealing temperature was previously tested by gradient PCRs.
The data was generated by using the *Biorad iQ5 iCycler* system. The data were normalized to different housekeeping genes like β2M (β2-Microglobulin) or GAPDH (Glycerinaldehyd-3-phosphat-Dehydrogenase) and was interpreted in accordance to the paper: "A new mathematical model for relative quantification in real-time RT-PCR" (*Pfaffl, M. W. 2001*). For the graphs, Excel and/or GraphPad Prism Software was used.

qPCR program:

Temperature (°C)	Time (s)	Cycles
95	180	1
95	3	NC
AT	20	NC
72	6	NC
60-95 melting curve	1	
20	∞	1

The primer annealing temperature (AT) as well as the number of cycles (NC) was dependent on primer pairs, determined by the gradient PCR.

qPCR Primer pairs:

Gene	Primer label	Sequence (5' – 3')	AT/NC	Company
L1TD1	h_L1TD1_F_set1	cttaccctggtagccgacct	56°C/	sigmaaldrich
	h_L1TD1_R_set1	ggctggcaaattttctaagg		
L1TD1	h_L1TD1_F_set2	gaaaatttgccagccaaaaa	56°C/	sigmaaldrich
	h_L1TD1_R_set2	gaagctcaagccatcactgg		
V5	h_V5_L1TD1 F1	tgtcttcaaagttctgctgga	64°C/	sigmaaldrich
	h_V5_L1TD1 R1	cctcatccccaagtacgcta		
V5	h_V5_L1TD1 F2	tgcccaccttgagagaattact	64°C/	sigmaaldrich
	h_V5_L1TD1 R2	attccttgctcctcatcccc		
GAPDH	h_gapdh F1	gtctcctctgacttcaacagcg	64°C/	sigmaaldrich
	h_gapdh R1	accaccctgttgctgtagccaa		

2.4.4 shRNA-mediated knockdown of L1TD1

Knockdown of the endogenous L1TD1 gene was performed using a set of two different siRNAs in OV-90 cells. For the knockdown experiment the cells were grown to 50% confluency on T25-flasks. For the transfection the Lipofectamine™ 2000 Transfection Reagent (*ThermoFisher)* or the PEI Transfection Reagent (*ThermoFisher*) was used, according to the manufacturer's handbook. For Lipofectamine, 0.5 ml Opti-MEM™ (*ThermoFisher*) and 10 µl of Lipofectamine 200 were incubated together in a 2 ml tube for 15 minutes at RT (under the hood). In the meanwhile, a second 2 ml tube with 0.5 ml Opti-MEM™ and 20 µl of 20 µM siRNA was prepared and incubated for 15 minutes at RT. After the incubation, the lipofectamine mixture was added to the siRNA mix and incubated together for an additional 20 minutes. Then the old cell media on the flasks was removed, the cells were washed twice with 1x PBS and 8 ml of new media without FBS was added. The transfection mix was dropwise added to the cells and incubated for 24 hours at 37°C. For the PEI transfection 100 µl of 150 mM NaCl was mixed and incubated for 15 minutes with 7 µl PEI at RT. Then 100 µl of 15 mM NaCl was mixed with 14 µl of the siRNA and incubated for 15 minutes. Afterwards the PEI mixture was carefully transferred to the siRNA mix and incubated on RT for 30 minutes. The rest of the protocol is similar to the Lipofectamine transfection. The cell media was removed, cells were washed, fresh FBS-free media was added and the transfection mixture was dropwise applied to the cells. After 24 and 48 hours the cells were harvested and the protein status of L1TD1 was checked via Western blotting. As control a scrambled siRNA, kindly provided by Heinz Fischer was used. The pre-designed silencer select L1TD1 siRNAs were ordered from *ThermoFisher.* Two different siRNAs were ordered, interfering with different exons of the L1TD1 genome.

Gene Symbol: L1TD1
Silencer™ Select Pre-Designed siRNA
Catalogue Number: 5392420
Unit size: 5 nmol
siRNA ID: s29244
Species: Homo sapiens

Gene Symbol: L1TD1
Silencer™ Select Pre-Designed siRNA
Catalogue Number: 5392420

Unit size: 5 nmol
siRNA ID: s29243
Species: Homo sapiens

2.5. Work with DNA

2.5.1. Isolation of genomic DNA from HAP-1 and OV-90 cells

For this purpose, the isolation of genomic DNAisolation kit (*Promega*) was used. Cells were harvested (*see section 2.1.5 Cell harvest*) and 600 µl of Nuclei Lysis Solution (provided in the kit) was added, resuspending the cells until no clumps remained. After that, 17.5 µl of 20 mg/ml Proteinase K (*Thermo Scientific*™) was added and the lysate was incubated for 3 hrs at 55°C on a shaker. The samples were vortexed once per hour. After incubation the samples were cooled down at RT and 200 µl of Protein Precipitation Solution was added and vortexed at high speed for 20 seconds. Then the samples were chilled on ice for 5 minutes. Centrifugation for 4 minutes at 13.523 rcf on RT followed. Then a tight white pellet should have formed (protein). The supernatant (DNA) was carefully removed and transferred to a clean 1.5 ml tube, containing 600 ml of isopropanol (RT). The solution was mixed by gently inverting the tube until a white-threat strand of DNA started to appear. Subsequently the DNA was centrifuged for 1 minute at 13.523 rcf at RT. DNA can be visualized as a small white pellet. The supernatant was carefully decanted. Then, 600 ml of 70% EtOH was added and the tube was gently inverted in order to wash the DNA. Afterwards centrifugation for 1 minute at 13.523 rcf at RT took place. The EtOH was carefully removed, and the DNA pellet was air dried for 10-15 minutes. In the last step 100 µl of DNA Rehydration Solution (provided in the kit) was added and the DNA was rehydrated for 1 hour at 65°C. The solution was periodically mixed by tapping the tube. The DNA was stored at 2-8°C. The DNA concentration was measured using NanoDropTM One C (*Thermo Fisher Scientific*).

2.5.2. Agarose gel electrophoresis

To confirm the amplification of the desired DNA fragment, the PCR product was loaded onto an agarose gel (concentration between 1.2-1.8%) and depending on the fragment size the DNA was separated. The agarose gel was prepared by mixing and boiling the SeaKem® LE Agarose powder (*Lonza Inc.*) in 100 ml 1x TAE buffer. In order to visualize the PCR product, peqGREEN DNA staining (*Peqlab*) was added to the gel after it cooled down a bit.

The *OneTaq® Quick-Load® 2X Master Mix* which was used, already containing the Loading buffer, was added to the PCR product. Around 7 µl of DNA ladder was added to one lane of the gel (depending on the DNA size you want to visualize), (*1 kb or 100 bp; NEB Inc.*). The gel ran for approximately 45 minutes at 90 V in 1x TAE buffer. After the run finished, the gel was visualized using the ChemiDoc XRS+ system (*Biorad*).

50x Tris-acetate-EDTA (TAE) buffer

242 g Tris-base
57.1 ml glacial acetic acid
100 ml 0.5 M EDTA
Filled up to 1 l with dH_2O and stored at RT.
pH adjusted to 8.0

3. Results

3.1. Characterization of the OV-90 cell line

In agreement with a report on the effect the DNMT inhibitor 5-aza-2′-deoxycytidine on L1TD1 expression *(Altenberger, C. et al. 2017),* we have recently found that loss of DNMT1 in the murine epidermis results in up-regulation of L1TD1 (Beck, Fischer *et al.* 2021). To test DNMT1-dependent regulation of L1TD1 in a cellular model we have generated HAP-1 DNMT1 KO and DNMT1/L1TD1 double knockout cell lines (Luisa Seufert, Master thesis, University of Vienna 2019). Indeed, loss of DNMT1 expression abolished the genetic silencing of L1TD1 in HAP1 cells (**Figure 18**). As a complementary approach, we wanted to analyze L1TD1 function in addition in a tumor cell line with natural expression of L1TD1. In collaboration with Wolfgang Sommergruber (Boehringer Ingelheim Vienna) we have previously analyzed human tumor cells for expression of L1TD1 RNA and protein. Only a small number of cell lines including the ovarian carcinoma cell line OV-90 (*Lounis, E. et al. 1998*) expressed higher levels of L1TD1 RNA and protein (**Figure 17** and data not shown).

Rank	S	Name	Tumor Type	Organ	Gender	TPM of L1TD1
1	☑	COR-L24	SCLC	lung	male	380
2	☑	D341 Med	medulloblastoma	brain	male	181
3	☑	ALL-SIL	hematopoietic/leukemia	peripheral blood	male	131
4	☑	OV-90	ovarian carcinoma	ovary	female	76.5
5	☑	DU4475	breast carcinoma	breast	female	67.5
6	☑	RPMI-8402	hematopoietic/leukemia	peripheral blood	female	65.5
7	☑	NCI-H2286	NSCLC	lung	female	29.5
8	☑	OUMS-23	colon carcinoma	colon		29.1
9	☑	CAL-120	breast carcinoma	breast	female	26.6
10	☑	NCI-H661	NSCLC	lung	male	26.1
11	☑	HD-MB03	medulloblastoma	brain	male	19.4
12	☑	EHEB	hematopoietic/leukemia	peripheral blood	female	19.2
13	☑	MHH-ES-1	bone sarcoma	bone	male	15.6
14	☑	RH-1	rhabdomyosarcoma	muscle	male	14.9
15	☑	GP2d	colon carcinoma	colon	female	13.5
16	☑	NCI-H2085	NSCLC	lung	male	12.1
17	☑	SK-N-MC	neuroblastoma	unknown	female	10.4
18	☑	COLO-680N	esophagus carcinoma	esophagus	female	10.2
19	☑	SK-ES-1	bone sarcoma	bone	male	9.82
20	☑	RD-ES	bone sarcoma	bone	male	9.34
21	☑	D283 Med	medulloblastoma	brain	male	8.46
22	☑	TMD8	hematopoietic/lymphoma	lymphatic system		8.33
23	☑	HuH-6		liver		6.73
24	☑	EKVX	NSCLC	lung	male	6.11
25	☑	A2780	ovarian carcinoma	ovary	female	5.93
26	☑	GP5d	colon carcinoma	colon	female	5.14
27	☑	BeWo	placenta carcinoma	placenta	male	4.71

Figure 17 | L1TD1 expression in human cancer cell lines. Transcriptome data were generously provided by Wolfgang Sommergruber, Boehringer Ingelheim Vienna.

Since L1TD1 expression is limited to only a few cell types including undifferentiated human embryonic stem cells and a small set of tumor cell lines, OV-90 cells were tested as a suitable model to study the function of L1TD1. To compare L1TD1 protein expression with previously characterized cell lines, we performed a Western blot analysis and used the DNMT1 knockout HAP-1 cell line (KO), as positive control and the DNMT1/L1TD1 double KO cell line (dKO), as a negative control.

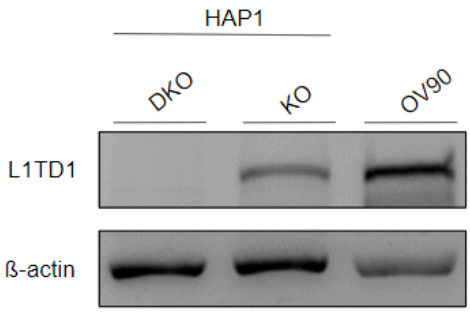

Figure 18 | Immunoblot analysis of L1TD1 in HAP-1 and OV-90 cells. cells were grown to 80-90% density, harvested, and proteins were isolated and loaded on a SDS-gel. The OV-90 cell line showed a higher expression of L1TD1 even though the loading control (ß-actin) showed that less of the OV-90 protein was loaded. The dKO cell line was used as a negative control.

As shown in **Figure 18**, OV-90 cells show a robust expression of L1TD1, which was slightly higher than in the HAP-1 KO cell line. Therefore, we decided to perform further experiments with OV-90 cells.

3.1.2. Localization of L1TD1

To support the Western blot results of the OV-90 cells, and to localize L1TD1 in these cells, an immunofluorescence analysis with an L1TD1-specific antibody was carried out.

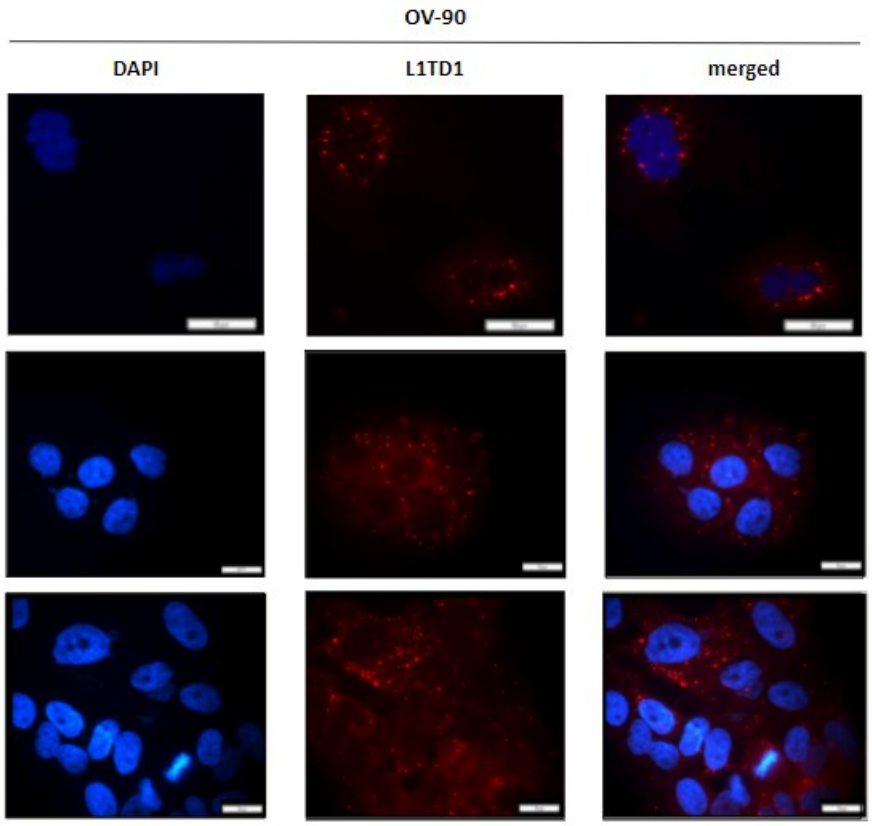

Figure 19 | Immunofluorescence detection of L1TD1 in OV-90 cells. The first column shows nuclear DNA staining with DAPI in blue. The second column shows the L1TD1 staining in red and the third column displays the merge of DAPI and L1TD1 staining. Scale bar: 10µm.

As shown in **Figure 19**, L1TD1 was clearly detectable in all DAPI positive cells and showed cytosolic localization. In accordance with previous results with HAP-1 cells and human ESCs, L1TD1 speckles in the cytoplasm were detected.

In order to compare the localization and strength of the L1TD1 signal between different cell lines, the HAP-1 dKO and KO cells were used for the next Immunofluorescence staining.

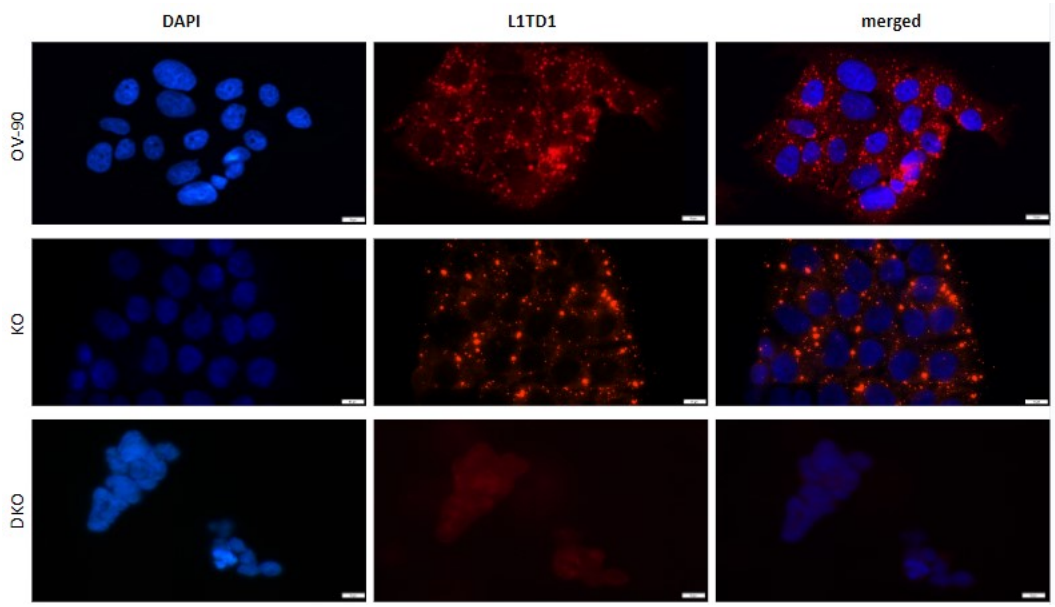

Figure 20 | Immunofluorescence detection of L1TD1 in OV-90 cells and HAP-1 cells. The first column shows the DAPI-stained nuclei of HAP-1 and OV-90 cells. L1TD1 expression in the cytoplasm is comparable in HAP-1 KO cells and OV-90 cells. The dKO cells shows only background signals for L1TD1. Scale bars: 10µm.

The immunofluorescence experiments with HAP-1 and OV-90 cells confirmed the localization of L1TD1 in the cytoplasm. Regarding the localization of L1TD1 in speckles, a previous study on L1TD1 in hESCs revealed that the protein co-localizes with P-bodies (*Närvä, E. et al. 2012*). In order to check this possible co-localization in HAP-1 and OV-90 cell lines, we decided to conduct an Immunofluorescence analysis with the P-body marker DDX6 (**Figure 20**).

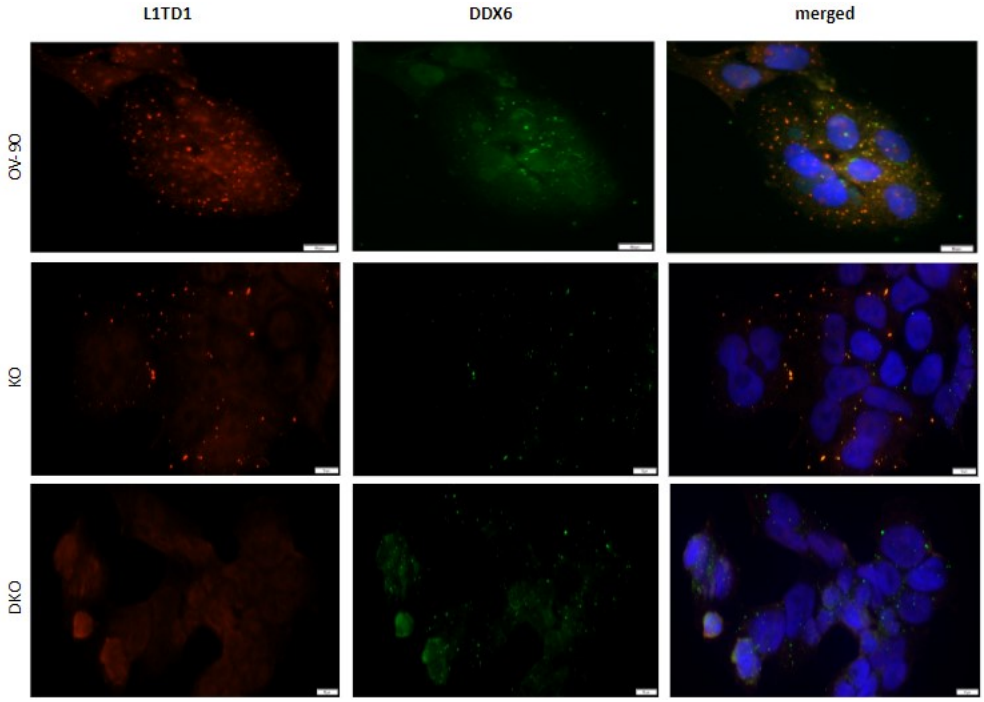

Figure 21 | Immunofluorescence detection of L1TD1 and P-bodies in OV-90 and HAP-1 cells. The first column shows L1TD1 in HAP-1 and OV-90 cells. The second column shows the P-body staining (DDX6) and the last column depicts the merged L1TD1 and P-body pictures. In all three cell lines P-body speckles were observable. In OV-90 and the KO cell line, the P-bodies partially overlap with the L1TD1 speckles in the cytoplasm. The DKO shows no L1TD1 staining. Scale bars: 10µm.

As shown in **Figure 21**, the P-body marker DDX6 showed a partial overlap with the L1TD1 speckles in the OV-90 and KO cell line. No clear differences in the overlap and the intensity and amount of the P-bodies were observable. These data suggest that both in HAP1-1 and OV-90 cells a subfraction of the L1TD1 speckles are P-bodies.

3.2. Generation of cell lines expressing a V5-tagged version of L1TD1 in the OV-90 cell line

In order to make future detection and purification of the L1TD1 protein easier, we decided to tag the L1TD1 protein with a C-terminal V5 epitope. To this end we created knock-in (KI) OV-90 cells using the CRISPR/Cas9 method.

OV-90 cells were transfected with a single-guide RNA (sgRNA), Cas9 endonuclease, and the HDR (homologue direct repair) DNA with the respective sequence for the V5-L1TD1 tag. The sgRNA guided the Cas9 endonuclease to the sequence of interest (L1TD1). Cas9, the endonuclease then made a cut at the targeted sequence and via the help of HDRs, the V5 tag was inserted in the exon 4 of the L1TD1 gene *(Ceasar, S. A. et al. 2016).*

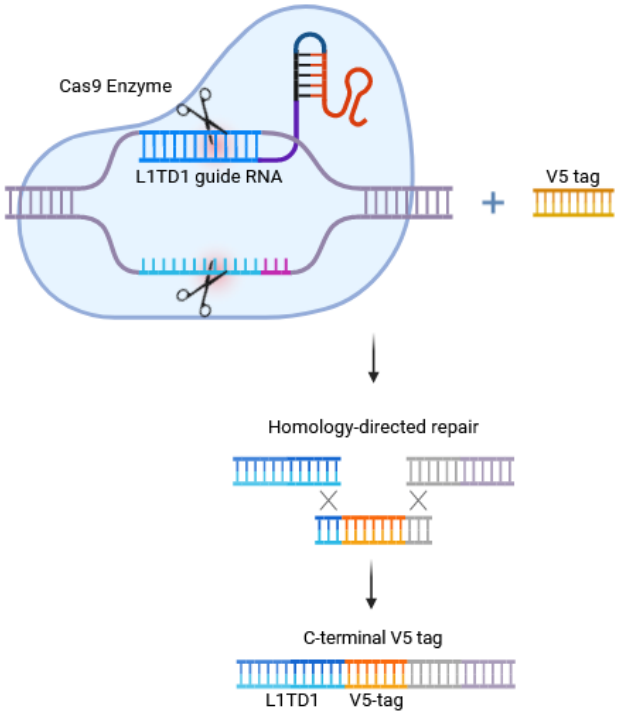

Figure 22 | The CRISPR/Cas9 genome editing mechanism. CRISPR/Cas9 is used for genome editing purposes, the sgRNA can be designed to specifically bind the target region, also known as protospacer. The Cas9 endonuclease recognizes the PAM sequence at the 3' end of the protospacer and induces a double-strand break (DSB). The CRISPR/Cas9 tool can be used for knock-in and knock-out experiments, depending on the used repair mechanism. *Via* homology direct repair the V5 sequence can get integrated into the desired genomic region. Figure taken from Fernández, C. R. (2021, November 3). CRISPR-Cas9: The Gene Editing Tool Changing the World.

To be sure that the transfection under the used conditions was efficient in OV-90 cells, a GFP plasmid was used as transfection control and showed ~ 20% fluorescence 2 days after electroporation. Since the introduced V5-tag DNA did not contain a GFP marker or antibiotic resistance gene, the identification of the V5-positive clones was carried out by Western blot analysis of single clones. In order to generate and identify single clones expressing V5-tagged L1TD1, limited dilutions of the electroporated cells were made. When the single cell clones reached suitable cell numbers, Western blot analysis was performed.

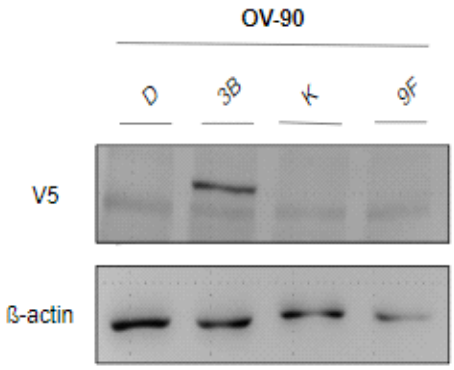

Figure 23 | Immunoblot analysis of possible positive V5 clones in OV-90 cells. D, 3B, K and 9F, all represent clones grown from single cells that underwent electroporation and were obtained by limited dilutions. Clone 3B gave a positive signal with the V5 antibody and the band displayed the expected size of the V5-tagged L1TD1 protein.

In order to be sure that the V5-positive signal actually represented the V5-tagged L1TD1 protein, a previously generated DNMT1 KO HAP-1 cell line expressing V5-tagged L1TD1 was used as a positive control for Western blot analysis. The HAP-1 V5-KI cell line 1D was kindly provided by Terka Vcelkova.

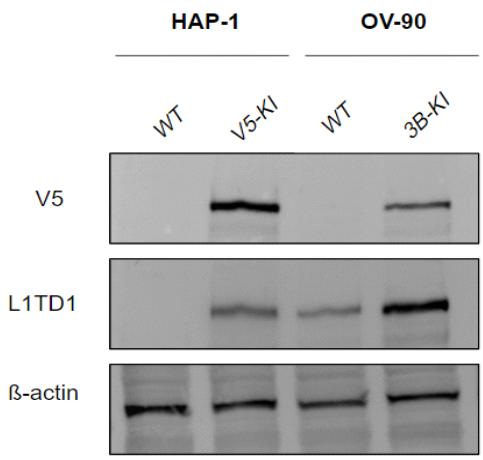

Figure 24 | Immunoblot analysis of positive V5-L1TD1 OV-90 cells. V5 knock-in in HAP-1 and OV-90 cells show the same V5-L1TD1 band and therefore confirm the results of our previous Western blot. HAP1 WT and OV-90 WT cells were used as negative controls.

The Western blot shown in **Figure 24** confirmed the expression of V5-tagged L1TD1 in the OV-90 clone 3B.

In order to confirm the V5-tag on the DNA level, DNA from the 3B cell line was isolated and the PCR product was analyzed on an agarose gel. As positive control the V5-tagged HAP-1 cell line 1D was used.

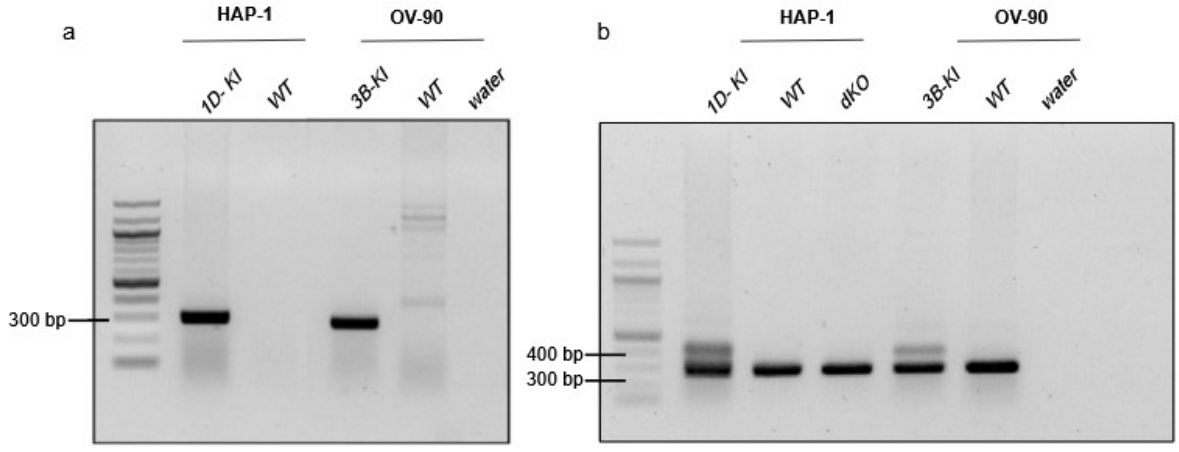

Figure 25 | Screening of positive clones with direct PCR method. In **panel a** a primer pair with one primer binding within the V5 tag is used (h_V5_L1TD1 F1/R1, expected product size ~ 298bp). In **panel b** a primer pair that binds to the left and to the right of the V5 tag is used (h_V5_L1TD1 F2/R2, expected product size ~ 423bp. The double bands in **panel b** for the KI cell lines show that the respective cell lines are heterozygous for the V5-tag.

Since the agarose gel in **Figure 25b** showed double bands in the two knock-in cell lines, we concluded that our cell lines were heterozygous for the V5-tag.

To check if the V5-tag allows to efficiently pull down L1TD1, an immunoprecipitation with V5-beads was carried out. For this experiment the OV-90 KI cell line 3B and OV-90 WT cells as negative control were used. As shown in **Figure 25**, the tagged L1TD1 protein was specifically precipitated. However, the amount of precipitated protein was relatively low. This might be due to the fact the cell line is heterozygous for the expression of V5-L1TD1.

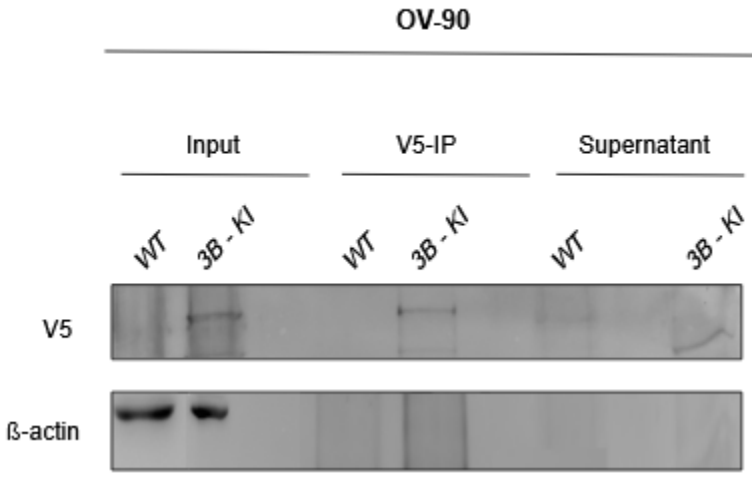

Figure 26 | Immunoblot analysis of the V5-IP. Protein extracts prepared from HAP1 wildtype cells (WT) and V5 KI 3B cells (3B-KI) and V5-tagged L1TD1 was precipitated with V5-beads. Input samples (20 µg), IP samples and aliquots of the supernatants were analyzed on a Western blot using the indicated antibodies.

Next, we tested the V5 antibody for the detection of tagged L1TD1 protein in immunofluorescence experiments.

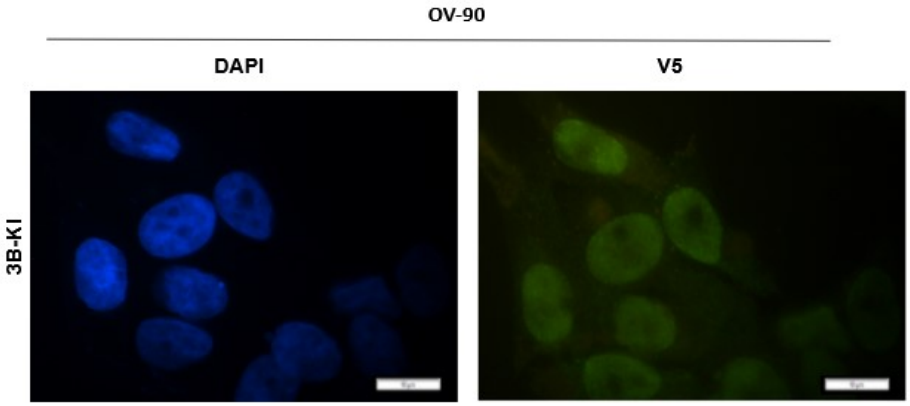

Figure 27 | Immunofluorescence detection of the V5-tagged L1TD1 protein in the 3B-KI cell line. Nuclear DNA was stained with DAPI and V5-L1TD1 was detected with V5-specific antibody. Scale bars: 10µm.

The V5 antibody gave a nuclear signal, what is in contrast to previous L1TD1 immunofluorescence experiments showing cytosolic localization of the wildtype protein. In addition, it was confirmed by Western blot analysis that the V5-tag is correctly fused with the L1TD1 protein. Therefore the V5 signal of the immunofluorescence experiment, shown in **Figure 27**, is probably caused by non-specific binding of the used V5 antibody.
The V5-tagged OV-90 cell line wasn't further used in this thesis but might be instrumental for future studies of the L1TD1 interactome in tumor cells.

3.3. Generation of HAP-1 cell lines with high expression of V5- L1TD1

As additional cell system for V5-tagging of L1TD1 we had also generated HAP1 KI cells expressing V5-tagged L1TD1. Unfortunately, we realized that longer cultivation of these cells led to reduction in the V5-tag signal. This is probably caused by a recurring repression of the L1TD1 gene upon longer cultivation. To overcome this problem limited dilutions from the V5-L1TD1 HAP-1 cell lines were made and the V5 expression was tested by Western blot analysis.

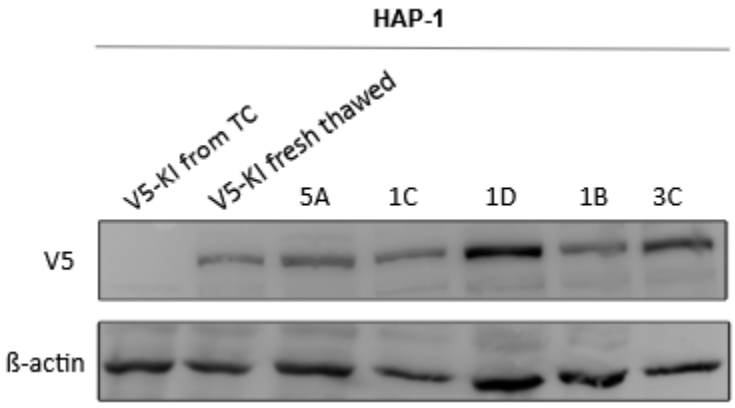

Figure 28 | Immunoblot analysis of the V5-tagged L1TD1 protein in HAP-1 cells. Cell extracts were prepared from V5-L1TD1 cells after long cultivation (first lane) or freshly thawed cells (second lane) and from single clones 5A, 1C, 1D, 1B and 3C obtained by limited dilution of the same cell line and probed with an L1TD1-specific antibody. ß-actin was used as loading control.

The Western blot shown in **Figure 28**, indicates that the expression of the V5-tagged L1TD1 in the long-cultured HAP-1 V5-KI cell line disappeared. By limited dilution, we were able to generate several HAP-1 cell lines with a higher V5 expression. To test if the strength of the V5 signal indeed varies in the different clones, especially for 1D and 3C, we repeated the Western blot analysis.

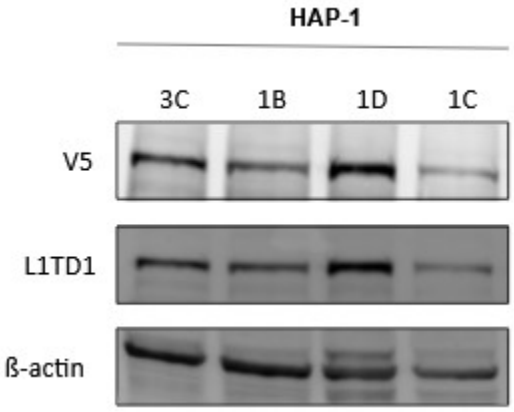

Figure 29 | Immunoblot analysis of the expression of V5-taged L1TD1 in HAP-1 cells. Cell extracts were prepared from V5-L1TD1 single clones 3C, 1B, 1D and 1C obtained by limited dilution of the same cell line and probed with an L1TD1-specific antibody. ß-actin was used as loading control.

The Western blot shows that the 3C and especially the 1D clone show stronger signals for the V5 and the L1TD1 protein (**Figure 29**). Therefore, we decided to continue with the 3C and the 1D clones, since both showed a constant and high V5 and L1TD1 expression on the Western blot.

3.4. L1TD1 interacts with a defined set of mRNAs and binds to its own transcript

To identify RNAs that are bound by L1TD1 RIP experiments were performed. As first step the efficiency of L1TD1 immunoprecipition (IP) with an L1TD1-specific antibody was tested. Unspecific IgG was used as negative control.

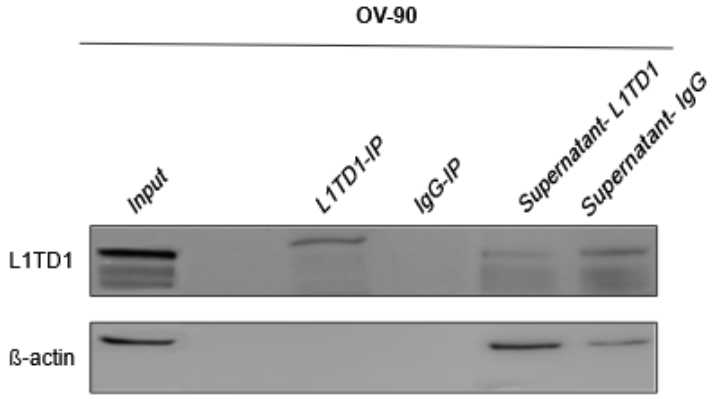

Figure 30 | Immunoblot analysis of the L1TD1-IP. Protein extracts prepared from OV-90 wild type cells. L1TD1 was precipitated with an L1TD1-specific antibody. IgG was used as negative control. Input samples (20 µg), IP samples and aliquots of the supernatants were analyzed on a Western blot using the indicated antibodies.

L1TD1 was specifically and efficiently immunoprecipitated although part of the protein remained in the supernatant. As expected immunoglobulin G (IgG) did not interact with L1TD1.

The next step was to check whether L1TD1 binds to L1TD1 RNA as described for human ESC (*Närvä, E. et al. 2012*). By L1TD1 RNA-immunoprecipitation followed by next generation sequencing in HAP-1 cells, my supervisor Gülnihal Kavaklioglu identified a set of RNA targets including L1TD1. Some of these hits including L1TD1 itself were confirmed by RIP combined with qRT-PCR (**Figure 31**).

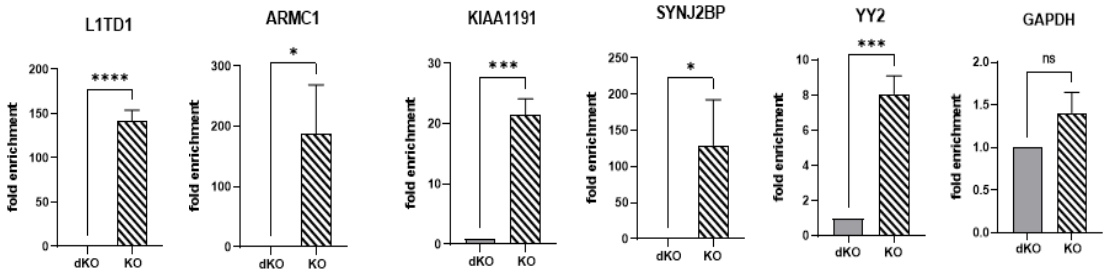

Figure 31 | Validation of L1TD1 RIP targets in HAP-1 cells. Selected L1TD1 targets including L1TD1 itself were confirmed by RIP combined with qRT-PCR. The HAP-1 L1TD1/DNMT1 DKO cell line was used as negative control for the IP and GAPDH was used as not bound control. Unpaired t-test, two-tailed. Error bars indicate SD. p-value <0.05. Figure kindly provided by Günihal Kavaklioglu.

The set of L1TD1-bound mRNAs included ARMC1,KIAA1191, SYNJ2BP and YY2. The function of the proteins encoded by selected target mRNAs differs strongly. ARMC1 is known to be involved in the intracellular distribution of mitochondria and possesses ion binding activity, while KIAA1191 is predicted to enable oxidoreductase activity (*NCBI n.d.*). SYNJ2BP is involved in several regulatory processes, like negative regulation of endothelial cell migration, negative regulation of sprouting angiogenesis as well as the regulation of signal transduction. It is an integral component of the mitochondrial outer membrane. YY2 on the other hand is a well-known transcription factor that is used as a positive and negative gene regulator since it possess both, activation and repressive domains (*NCBI n.d.*).

The strongest binding of L1TD1 was observed for its own transcript. Therefore, an RNA-Immunoprecipitation for L1TD1 was also carried out in the OV-90 cell line. The result shown in **Figure 31** proved that L1TD1 interacted with its own transcript also in OV-90 cells.

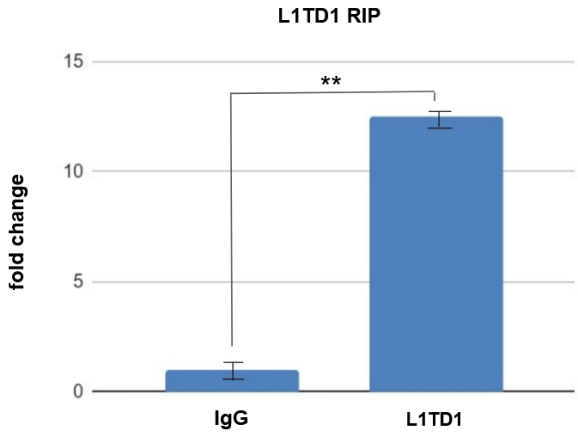

Figure 32 | L1TD1 protein binds to its own mRNA in OV-90 cells. A RIP experiment was performed with extracts isolated from OV-90 cells using an L1TD1-specific antibody and IgG as negative control. Levels of bound L1TD1 transcripts were determined by qRT-PCR. P = 0.0151, Unpaired t test, two-tailed. Error bars indicate SD.

The interaction of L1TD1 with specific RNAs, in particular with its own transcripts, was thereby confirmed.

3.5. L1TD1 interacts with other proteins over RNA molecules.

L1TD1 binds to its own transcript, which we previously showed after performing an RNA-immunoprecipitation in OV-90 and HAP-1 cells. Now that its RNA-binding ability was confirmed, we wanted to find out about other proteins that might interact with L1TD1 directly or *via* bound RNA molecules. To do this, a V5-beads immunoprecipitation of HAP-1 cells with and without subsequent RNase treatment, was carried out. After separation of the proteins by SDS-PAGE, the gel was stained using the silver staining protocol.

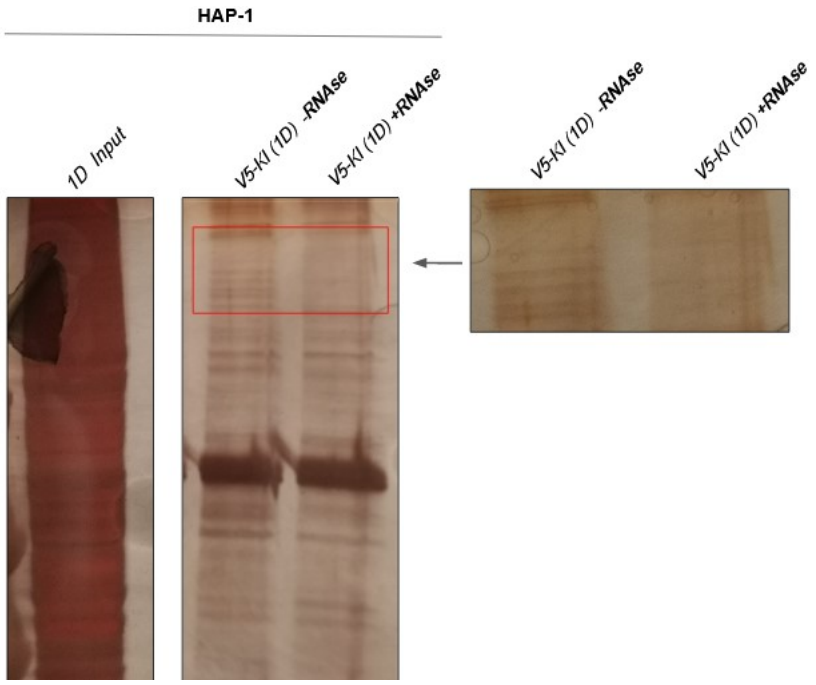

Figure 33 | Effect of RNase treatment on L1TD1-interacting proteins in HAP-1 cells. Cell extracts from V5-L1TD1 expressing cells (V5-KI 1D) were immunoprecipitated with V5-beads and half of the IP sample was treated with RNase. An input aliquot and the IPs were separated on a SDS polyacrylamide gel and silver-stained. The zoom-in shows that specific protein bands are sensitive to RNase treatment (arrow).

Interestingly, some of the co-precipitated proteins disappeared upon RNase treatment suggesting that these proteins interact *via* binding to RNA molecules (**Figure 33**). These results are of interest for future mass spectrometry analysis of the L1TD1 interactome in tumor cells.

3.6. L1TD1 loss affects the proteome and transcriptome of HAP-1 cells

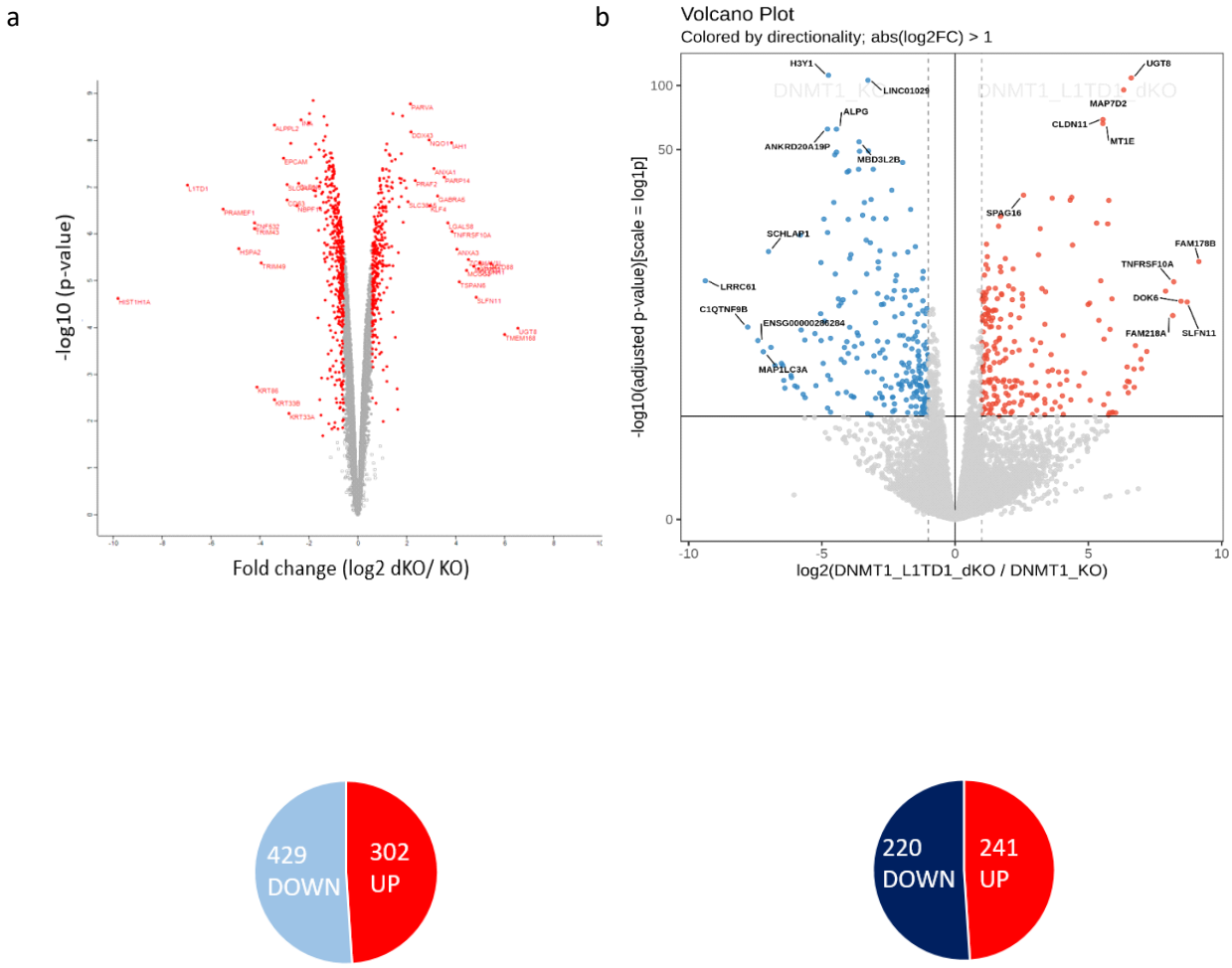

Figure 34 | Mass-spectrometry and RNA-sequencing analysis of HAP-1 dKO and KO cell lines. Volcano plot analysis of changes in the expression of RNA (**panel a**) or protein (**panel b**). In both analyses significant changes in response to loss of L1TD1 are visible. The Figure was kindly provided by Gülnihal Kavaklioglu. **Panel a**: p-value: <0.05, abs(log2FC) > 0.585; **Panel b:** p-value: <0.05, abs(log2FC) > 1.

Given that L1TD1 interacts with a specific set of RNAs, we wanted to examine potential effects of L1TD1 on the abundance of RNAs and proteins in HAP1 cells. In order to compare the transcriptomes and proteomes, we sent samples of KO and dKO HAP-1 cells for mass spectrometry and RNA sequencing analysis.

The RNA-seq analysis showed a deregulated subset of genes in the absence of L1TD1 (**Figure 34a**). Furthermore, mass spectrometry analysis of HAP-1 cells indicated, that the loss of L1TD1 leads to a differential proteome in DNMT1/L1TD1 dKO cells in comparison to DNMT1 KO HAP1 cells (**Figure 34b**) (data kindly provided by Gülnihal Kavaklioglu).

Since L1TD1 is expressed in HAP-1 cells only upon DNMT1 knockout, we intended to study the effect of L1TD1 ablation in a cell line that naturally expresses L1TD1 (OV-90). To achieve that, the generation of a L1TD1 knockout cell line in OV-90 cells would be instrumental.

3.7. Attempts to generate OV-90 L1TD1 Knockout and Knockdown cell lines

In order to investigate possible L1TD1 RNA and protein interactions in a seond cell system and to also get a better understanding of its role in ovarian cancer cells, a knockout using CRISPR/Cas9 and a knockdown using siRNA was carried out in OV-90 cells. We have chosen OV-90 cells, since they are one of the very few cell lines naturally expressing L1TD1.

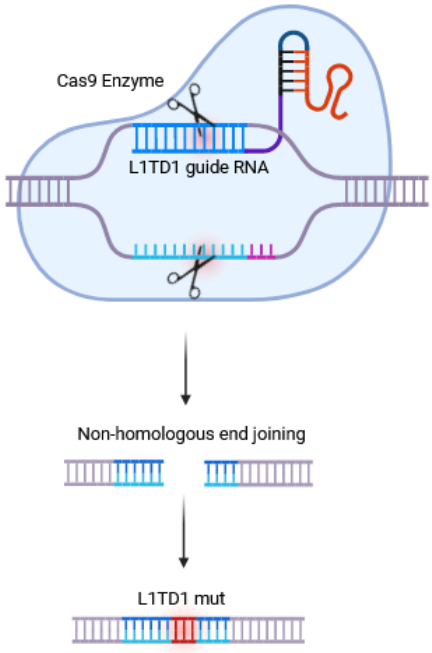

Figure 35 | Producing a L1TD1 KO cell line using the CRISPR/Cas9 genome editing system. The sgRNA that is directed against the L1TD1 gene leads the Cas9 endonuclease to the target sequence. Cas9 recognizes the PAM sequence at the 3' end of the protospacer and induces a double-strand break (DSB). Without the addition of a template DNA with homologues arms a random DNA repair process called non-homologous end joining jumps in and closes the induced double strand break. This mechanism often leads to a subset of mutations that can alter the function of the gene. In our cell line, part of the exon 4 of L1TD1 was the target of the guideRNA. The Knockout would ideally delete around 13bp and therefore lead to a non-functional gene. *CRISPR-Cas9: The Gene Editing Tool Changing* the World. Figure created with *BioRender.com*.

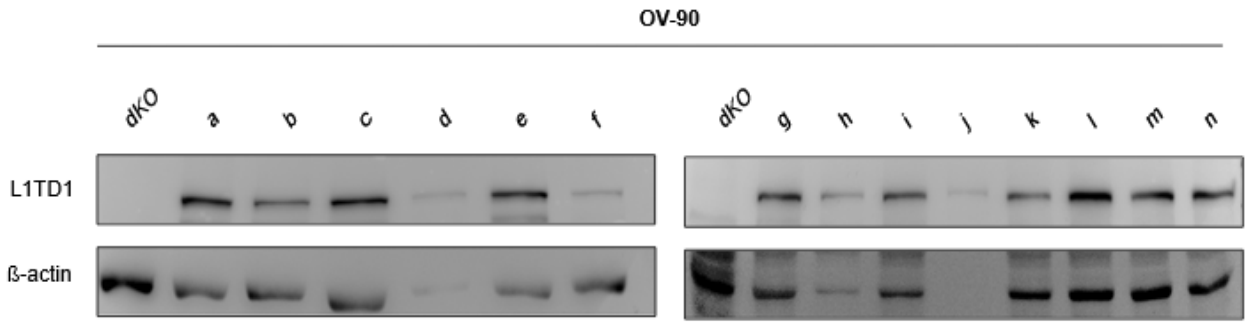

Figure 36 | Immunoblot analysis of the L1TD1 knockout attempts. CRISPR/Cas-9 mediated gene editing was performed as described in *Materials and Methods* and cell lysates of single clones were analyzed on Western blots for the presence of L1TD1 protein. The HAP-1 DKO cell line was used as control. ß-actin was used as loading control.

To target the sequence in the knockout, a L1TD1-specific gRNA that was already successfully applied for the L1TD1 KO in HAP1 cells was used (5'-tgatgaaaggtcggctacca-3'). As transfection control we used a GFP plasmid that showed a 10% transfection efficiency 2 days after transfection. Single clones were generated by limited dilution and tested for loss of L1TD1 protein. All together 40 clones were checked but unfortunately no knockout clones were obtained (see a representative Western blot analysis in **Figure 36**). Therefore, we decided to perform a knockdown experiment, which was easier to carry out and less time consuming.

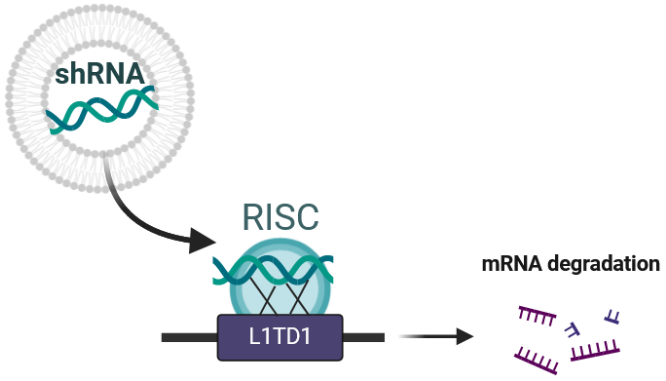

Figure 37 | siRNA mediated knockdown. The transfection agent, a liposome, fuses with the cell membrane and deposits the siRNA. The RISC complex binds to the siRNA and the mRNA of the target sequence, activates its RNase and cleaves the miRNA of L1TD1 (Pratt, A. J. et. al. 2009). Figure created with *BioRender.com*.

For the knockdown, two different shRNAs, which were specific for the human L1TD1 gene were used. Two different transfection agents, Lipofectamine and PEI, were used. Two and five days

after the conducted transfection, the L1TD1 expression of the cells was checked. As control a scrambled siRNA was used.

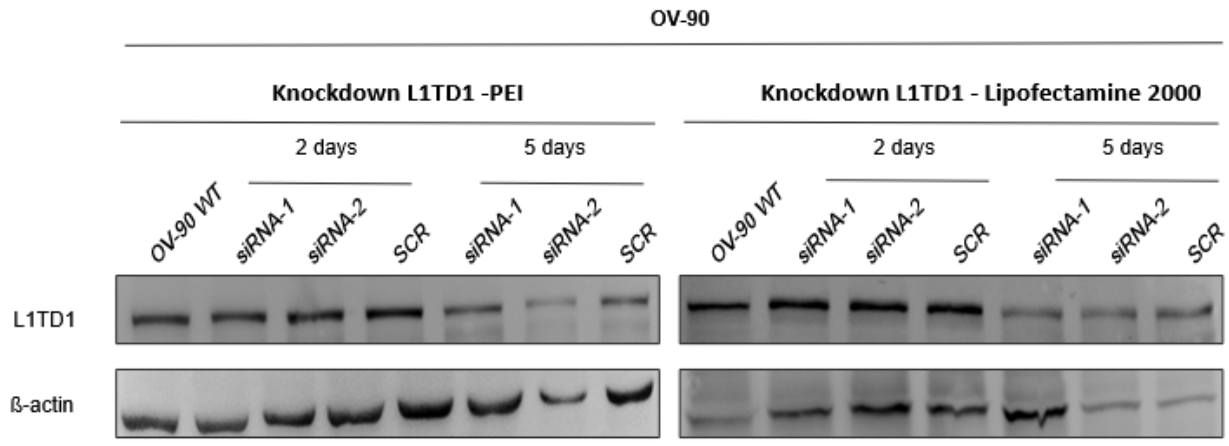

Figure 38 | Immunoblot analysis of the L1TD1 knockdown attempts. L1TD1 knockdown was performed with two different siRNAs and scrambled RNA (SCR) as negative control. Cells lysates were generated and analyzed on Western blots for presence of L1TD1 protein. ß-actin was used as loading control.

Both experiments failed and we were never able to generate a full knockout or knockdown. Even after additional knockdown experiments by me and my colleague, Dr. Heinz Fischer, we didn't manage to get an L1TD1 KO or KD.

3.8. L1 ORF1p upregulation in the absence of L1TD1

The proteome analysis of HAP-1 KO and dKO cell-lines described in *Chapter 3.6* revealed a slight but significant up-regulation of the LINE-1 ORF1p protein. L1 ORF1p is known to bind to different proteins and RNAs (*Mita, P. et. al. 2018*). In order to validate the up-regulation of ORF1p, we performed Western blot analyses.

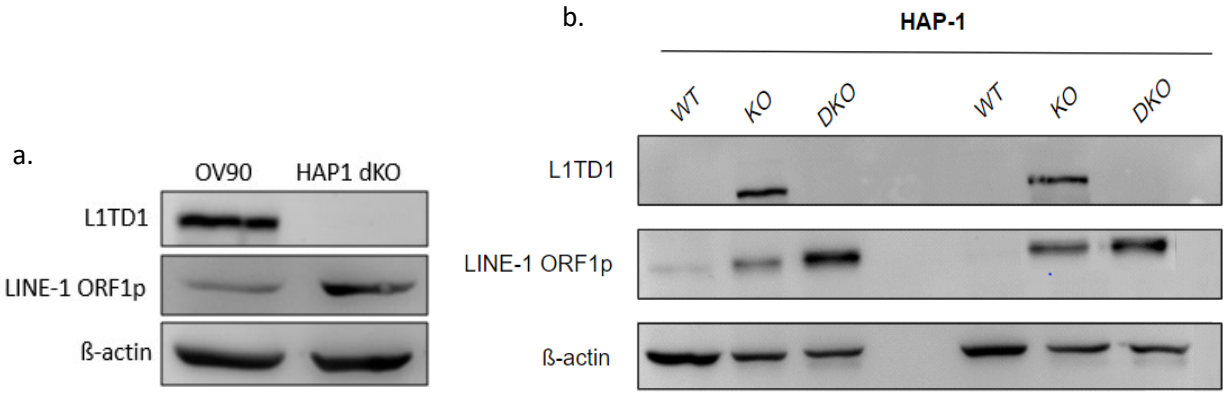

Figure 39 | Immunoblot analysis of the L1TD1 and L1 ORF1p expression in HAP-1 and OV-90 cells. Cell extracts prepared from OV-90 and HAP-1 KO cells (**panel a**) and two different batches of HAP-1 wildtype (WT), KO and dKO cells (**panel b**) were prepared and examined by Western blot analysis with the indicated antibodies. ß-actin was used as loading control. The Figure shown in **panel a,** was kindly provided by Gülnihal Kavaklioglu.

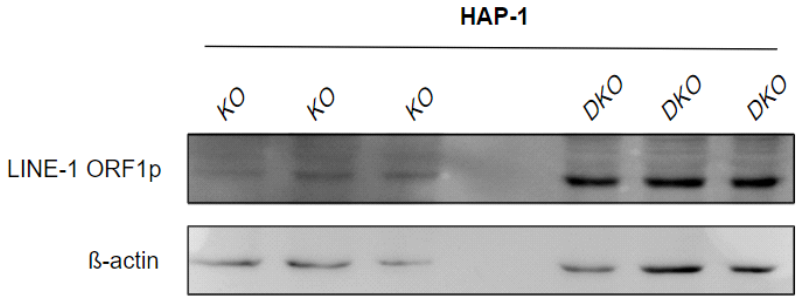

Figure 40 | Immunoblot analysis of LINE-1 ORF1p expression in HAP-1 KO and dKO cells. The triplicate biological replicas of HAP-1 KO and dKO cell lines used for the proteome analysis were tested on the Western blot for LINE-1 ORF1p expression. ß-actin was used as loading control.

The results of the two Western blots shown in **Figures 39** and **40** matched. LINE-1 ORF1p proteins was expressed at a higher level in the absence of L1TD1.

3.9. Interaction of L1TD1 and L1 ORF1p

To test if L1TD1 and L1 ORF1p interact not only functionally but also physically co-immunoprecipitation experiments were carried out. Given the higher L1TD1 expression, the OV-90 WT cell line was used first for this experiment.

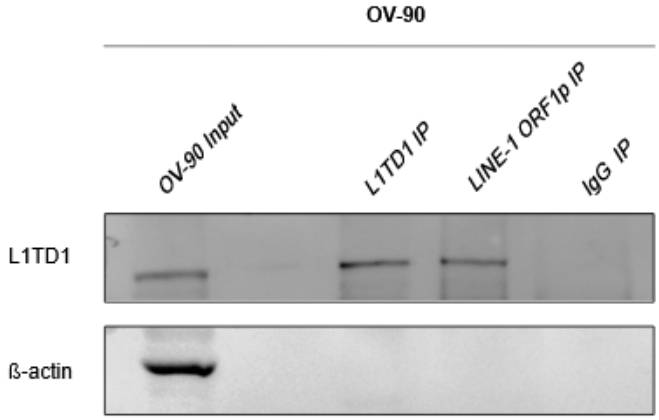

Figure 41 | L1TD1 co-immunoprecipitates with LINE-1 ORF1p. Protein extracts from OV-90 cells wer used for immunoprecipitation with antibodies specific for L1TD1 or L1 ORF1p: IgG was used as negative control. An input aliquot and the IPs were analyzed on a Western blot for presence of L1TD1. ß-actin was used as loading control.

Interestingly, the L1TD1 protein was present not only in the L1TD1 IP but also in the LINE-1 ORF1p IP but not in the IgG control IP. Unfortunately, the LINE-1 ORF1p antibody used for these Western blots stopped working at this point and I couldn't show the same interaction in the L1TD1 IP. Subsequent IPs/RIPs were carried out by my supervisor Gülnihal Kavaklioglu who then confirmed the pull-down of L1TD1 in the LINE-1 ORF1p IP in HAP-1 cells and furthermore showed their interaction on the RNA level, see (**Figure 42**).

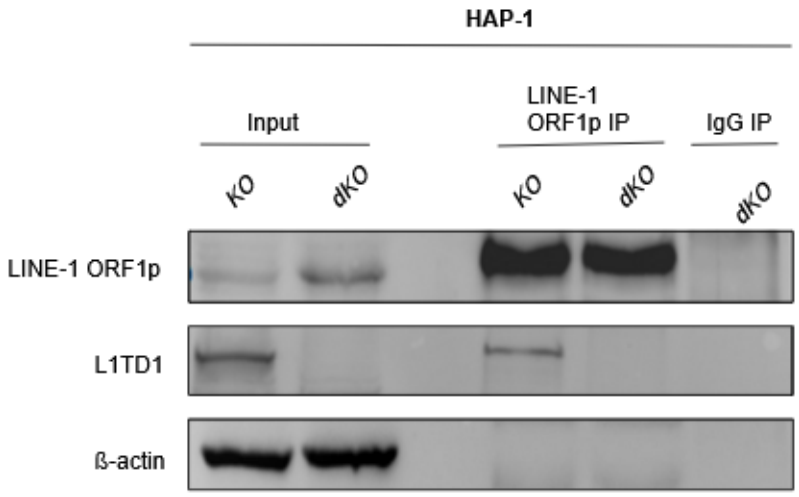

Figure 42 | L1TD1 associated with LINE-1 ORF1p in HAP-1 cells. Proteins were extracted from OV-90 cells and immunoprecipitated with antibodies specific for L1TD1 or L1 ORF1p: IgG was used as negative control. An input aliquot and the IPs were analyzed on a Western blot for presence of L1TD1 and L1 ORF1p. ß-actin was used as loading control. This figure was kindly provided by Gülnihal Kavaklioglu.

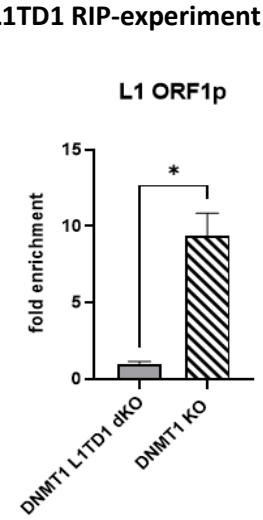

Figure 43 | Pull down of LINE-1 ORF1p mRNA in an L1TD1 RIP experiment in HAP-1 KO cells. A L1TD1 RIP experiment was performed with HAP-1 KO cells and dKO cells and analyzed for the presence of L1 ORF1p RNA by qRT-PCR. Unpaired t-test, two-tailed. Error bars indicate SD; P <0.05. The figure was kindly provided by Gülnihal Kavaklioglu.

Furthermore showed in RIP qRT-PCR experiments that L1TD1 protein binds not only its own mRNA but also LINE-1 RNA (**Figure 43**).

Our IP and RIP results showed a clear interaction between L1TD1 and its ancestor LINE-1 ORF1p. This, together with the upregulation of LINE-1 ORF1p on the protein level in L1TD1 KO cells, supports the assumption that L1TD1 might regulate LINE-1 expression/activity.

3.10. Co-localization of LINE-1 and L1TD1 proteins

After showing that L1TD1 and LINE-1 have the ability to interact and influence each other, a last experiment to support these results was conducted. In order to interact with each other L1TD1 and LINE-1 have to localize in proximity to each other. To show this potential co-localization, an Immunofluorescence was performed. Antibodies against L1TD1 and LINE-1 ORF1p were used in this context.

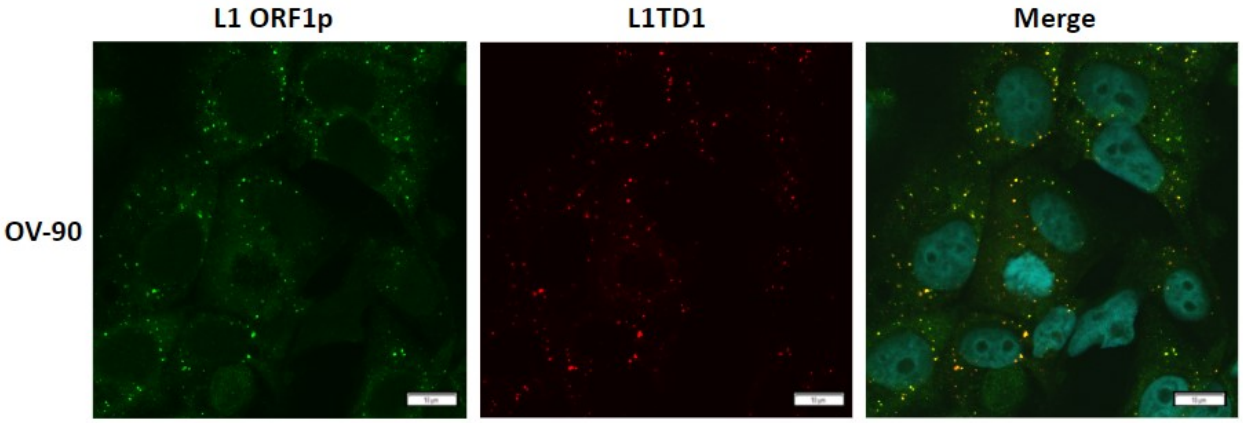

Figure 44 | Immunofluorescence analysis of L1TD1 and LINE-1 ORF1p in OV-90 cells. L1 ORFp shown in green and L1TD1 in red. DNA was stained with DAPI.

The indirect immunofluorescence analysis confirmed the cytosolic localization of L1TD1 and LINE-1 ORF1p in OV-90 cells. Both proteins show speckle-like signals with partial co-localization.

Taken together our study demonstrates that L1TD1 and its ancestor protein ORF1p physically and functionally interact in human tumor cells.

4. Discussion

4.1 Successful generation of a V5-L1TD1 fusion protein in OV-90 cells

The function of the L1TD1 protein has not been discussed much in literature. Therefore, the pool of possible antibodies for different experiments is limited. To enable easier, faster and more precise work we decided to generate a V5-tagged version of the L1TD1 protein. This V5-tag functions as a universal epitope that can be easily detectable by commercially available antibodies. In general, it should not compromise the native structure or function of the protein, but this can only be fully confirmed by directly comparing wildtype and V5-tagged L1TD1 in functional assays such as RIP. The V5-tag was nicely detectable in our performed Western blots. Unfortunately, the V5-IPs we performed showed only low V5 and L1TD1 signals. For comparison a follow-up IP was done, this time using only an L1TD1-specific antibody. The output of the L1TD1 antibody IP, showed much higher L1TD1 amounts in the Western Blot, compared to the V5-IP. A possible explanation is that only half of the L1TD1 proteins are tagged with the V5 epitope. Another reason might be that there is a difference between the binding efficiency of the V5 beads and the L1TD1 antibody. To save time we switched to another V5-tagged cell line, the HAP-1 V5-KI cell line. By time this cell line also started showing a V5-tag loss. This is most probably due to a reestablished repression of the L1TD1 gene in the HAP-1 KO cell line. This was a general phenomenon observed for the DNMT1 deficient cell line. In order to regain the expression of V5-tagged L1TD1 in the HAP-1 cell line, limited dilutions were made, and we were able to enrich the V-5 tagged cells. Two HAP-1 cell lines with high V5-L1TD1 expression were created, 1D and 3C, and stored for further experiments at -150°C.

4.2 RNA based protein interaction of L1TD1

In agreement with previous publications our experiments showed a strong interaction of L1TD1 with its own transcript (*Närvä, E. et al. 2012*). With the performed L1TD1 RNA-Immunoprecipitation experiments we were able to identify a set of additional RNA targets of L1TD1 and therefore confirmed its RNA-binding ability in HAP-1 and OV-90 cells.

By performing a silver staining of an L1TD1 IP, we were also able to see that the addition of RNAse led to a reduced protein pulldown. This indicates that L1TD1 is partially interacting with different proteins over bound RNAs. Previous studies on L1TD1 already showed an interaction

with LIN28, U2af1 and Srsf3 *via* RNA (both important for somatic cell reprogramming) (*Närvä, E. et al.2012*). In general, a large interaction network of L1TD1 is suspected, which is not only based on its RNA-bindingfunction, but also on its direct protein complex formation ability (*Närvä, E. et al. 2012*). It was furthermore shown that proteins like OCT4, SOX2, and NANOG directly bind to the promoter of L1TD1 (*Närvä, E. et al. 2012*). There is also the hypothesis that L1TD1 forms a protein complex with RHA (RNA helicase A) and LIN28 (*Närvä, E. et al. 2012*), (*Emani, M. R. et al. 2015*). The fact that L1TD1 partially co-localizes with P-bodies in our immunofluorescence experiments also indicates its role as a possible RNA regulator, since P-bodies play an essential role in mRNA decay (*Närvä, E. et al. 2012*).

The actual interaction platform for many of the potential interaction partners of L1TD1 is still unknown. Whether L1TD1 interacts more *via* direct protein binding or via RNA remains to be explored. Also, the strength of possible interactions needs to be further investigated, since RNAs bound to L1TD1 with low affinity tend to fall off and get lost in the IP process.

4.3. Interaction of L1TD1 and LINE-1 ORF1p

To check if there is a direct interaction between L1TD1 and its ancestor L1 ORF1p, a co-IP using L1TD1 and L1 ORF1p antibodies was carried out. We were able to see that L1TD1 was also pulled down in the LINE-1 IP and *vice versa*. These results indicated that the proteins interact with each other on the protein level. A potential explanation would be that their interaction is based on bound RNAs such as the LINE-1 transcript. In agreement with this idea, the ability of L1TD1 to bind LINE-1 ORF1p RNA was shown by L1TD1 RNA-IP. Whether their interaction is entirely dependent on RNA molecules needs to be further investigated.

4.4. L1TD1 expression correlates with LINE-1 ORF1p downregulation

The linkage between L1TD1 and LINE-1 poses many questions. LINE-1, as a highly active transposon and binds to many different RNAs. It provides the machinery for transposition of many non-autonomous elements *(McLaughlin, R. N., Young, J. M., et.al. 2014*). Since L1TD1 is a descendant of LINE-1 and shares high sequence similarity with the ORF1 of the LINE-1 element (exon 1 and exon 2, share 30% and 43% amino acid identity to their ancestor gene ORF1), we wanted to investigate their potential regulatory interaction (*McLaughlin, R. N., Young, J. M., et.al. 2014*). Western blot analysis of the HAP-1 DNMT1 KO cell line and the HAP-1 DNMT1/L1TD1 dKO cell line showed a very interesting expression pattern. It seemed that upon L1TD1 loss, the LINE-1 expression increased. This correlation might already indicate that L1TD1 and LINE-1 are interacting with each other. Since the L1TD1 gene possesses the repeated, putative LINE-1 RNA-binding domain, binding between them is possible *(Chiu, C. C. et al. 2017).* After analyzing and comparing the proteome and the transcriptome of the HAP-1 KO and the dKO cell line a deregulation of a subset of genes and RNAs indicated the potential regulative role of L1TD1.

L1TD1 could function as a LINE-1 restriction factor, maybe by interfering with the homotrimerization of the L1-ORF1 protein, which is necessary for its retrotransposition (*McLaughlin, R. N., Young, J. M., et.al. 2014).* On the other hand, L1TD1 could also outcompete L1 ORF1p for the binding to the ORF2p protein, leading to less LINE-1 retrotransposition. There is also the possibility that L1TD1 acts upstream of LINE-1 and reduces its expression *via* other proteins or RNAs. L1TD1 might affect the translation efficiency and/or protein stability of L1 ORF1p and this needs to be investigated further.

4.5. L1TD1 as a difficult knockout/knockdown target

One aim of my Master thesis was the set-up of an L1TD1 Knockout or Knockdown. To establish an authentic model system we worked with the naturally expressing L1TD1 cell line OV-90. Since L1TD1 is known to be involved in the post-transcriptional regulation in human pluripotency in nuclear traffic and proteasomal activity we assumed a reduced L1TD1 expression or a general loss of L1TD1 is going to have some effects on proteins being involved in these processes

(*Emani, M. R. et al. 2015*). Furthermore, the upregulation of L1TDT in various cancer cells as well as during pluripotency highlighted its importance in the cell (*Chakroborty, D. et al 2019*). Our goal was to examine possible effects on the protein, RNA or DNA level in the OV-90 cell line upon L1TD1 loss or downregulation. After several failed attempts of creating a knockout or a knockdown we stopped the experiments. We were able to perceive a reduction of L1TD1 in some clones, but never created a full knockdown or knockout. Many single colonies/cells died in the process of limited dilution, which led us to the assumption that OV-90 might be dependent on L1TD1 activity and reacted very sensitive to its loss. The cells in general developed a very slow growth pattern after diluting them, it took up to one month until small single colonies were observable under the microscope. L1TD1 is described as a cancer biomarker (*Chakroborty, D. et al. 2019*), therefore it might be possible that the cancer cell line is dependent on the L1TD1 expression. If the cells are then exposed to an additional stress like missing cell contact/communication, while performing limited dilutions, it could be possible that these conditions (L1TD1 loss and missing cell contact) were too stressful for the used cell line and therefore didn't work.

Since there is no available data on a successful L1TD1 KO in cancer cells, we suspect that L1TD1 is essential for the OV-90 cell growth and survival. The general manipulation of L1TD1 levels already seemed to be problematic. Various knockdown experiments in our study only led to a slight change in L1TD1 expression. Even the introduction of the V5-tagged L1TD1 version in OV-90 cells already caused problems. Cell growth seemed to be reduced and other experiments with this cell line didn’t work (Immunofluorescence) or gave us a poor output (V5-IP). To strengthen our assumption, further knockdown/knockout experiments on OV-90 cells under optimized conditions should be carried out.

4.6. L1TD1 as a potential target for chemotherapy

As described in the introduction, L1TD1 and LINE-1 expression is often associated with different cancer forms (*Xiao-Jie, L. et al. 2016), (Altenberger, C. et al. 2017).* The silencing of the LINE-1 element is a critical step to maintain genomic stability, since more active and jumping LINE-1 elements lead to a higher transposon rate which can be associated with the rise of new mutations due to unfavorable integration events (*Chiu, C.-C. et al. 2017).* LINE-1 is present in almost all epithelial cancers and highly expressed in stem cells (*McKerrow, W. et al.2023*). Our performed Western blots showed that in the absence of L1TD1, LINE-1 is upregulated, which in

the end might again lead to a higher transposon rate resulting in more mutation events and the development of cancer. To use L1TD1 as an LINE-1 inhibiting protein, in the fight against cancer might be an option. Furthermore, a frequent downregulation of the L1TD1 mRNA expression in primary tumor samples was found (*Altenberger, C. et al. 2017*). These low L1TD1 amounts might promote higher LINE-1 retrotransposition events, which could originally be one of the factors causing cancer. Increased L1TD1 expression is used as a positive marker with longer disease-free survival in colon cancer (*Chakroborty, D. et al. 2019*). These findings highlight the role of L1TD1 as a novel therapeutic target. Interestingly in some other cancer types, like medulloblastomas, high L1TD1 levels were correlated with a poor diagnosis (*Chakroborty, D. et al. 2019*). In general, L1TD1 expression is restricted to few cancer types and its effects (LINE-1 suppressing properties) need to be investigated further (*Expression of L1TD1 in cancer - Summary. (n.d.)).*

5. Outlook

To clarify if the L1TD1 and LINE-1 ORF1p interaction is RNA based, additional Co-IP experiments in the presence and absence of RNAse, is advisable. Since the interaction between L1TD1 and LINE-1 gets more visible through our experiments on HAP-1 cells, creating an inducible L1TD1 knockout/knockdown cell line in OV-90 should be tried. After the successful creation of a L1TD1 OV-90 knockout cell line, the LINE-1 expression with and without L1TD1 can be compared to the results of the HAP-1 KO and DKO experiments. Upon L1TD1-KO it might also be interesting to have a look at the actual changes of the protein composition between knockout and wildtype using Mass Spectrometry. Then the search for possible interaction targets of L1TD1 and LINE-1 can be carried out by additional RIP experiments and qRT-PCRs. To check if the actual transposon rate, caused by LINE-1, is being reduced upon L1TD1 loss, a retrotransposition assay can be carried out too. Thereby we would be able to see if the reduced LINE-1 expression also leads to a decrease of retrotransposon activity.

Since V5-tagged version of L1TD1 are available in HAP-1 and OV-90 cells interactome studies by mass spec analysis could be performed. This would allow to compare the spectrum of interactors published in hESCs with the one in tumor cells.

Further research on the expression and interaction of L1TD1 and LINE-1 ORF1p will hopefully generate a new basis for the classification and potential treatment of different cancer types. Since LINE-1 elements have the ability to enhance genomic instability, which is one of the hallmarks of cancer pathogenesis, their regulation on the cellular level needs to be understood (*Xiao-Jie, L. et al. 2016*). If L1TD1 represents such a potential LINE-1 regulator, it might be a valuable target for anti-cancer drugs.

References

Altenberger, C., Heller, G., Ziegler, B., Tomasich, E., Marhold, M., Topakian, T., Müllauer, L., Heffeter, P., Lang, G., End-Pfützenreuter, A., Döme, B., Arns, B. M., Klepetko, W., Zielinski, C. C., & Zöchbauer-Müller, S. (2017). SPAG6 and L1TD1 are transcriptionally regulated by DNA methylation in non-small cell lung cancers. Molecular Cancer, 16(1). https://doi.org/10.1186/s12943-016-0568-5

Anwar, S. L., Wulaningsih, W., & Lehmann, U. (2017). Transposable Elements in Human Cancer: Causes and Consequences of Deregulation. International journal of molecular sciences, 18(5), 974. https://doi.org/10.3390/ijms18050974

Barrero, M. J. (2020). Epigenetic Regulation of the Non-Coding Genome: Opportunities for Immuno-Oncology. Epigenomes, 4(3), 22. MDPI AG. Retrieved from http://dx.doi.org/10.3390/epigenomes4030022

Beck, C. R., Garcia-Perez, J. L., Badge, R. M., & Moran, J. V. (2011). LINE-1 elements in structural variation and disease. Annual review of genomics and human genetics, 12, 187–215. https://doi.org/10.1146/annurev-genom-082509-141802

Biémont, C. (2010). A brief history of the status of transposable elements: From junk DNA to major players in evolution. In Genetics (Vol. 186, Issue 4, pp. 1085–1093). https://doi.org/10.1534/genetics.110.124180

Burns K. H. (2017). Transposable elements in cancer. Nature reviews. Cancer, 17(7), 415–424. https://doi.org/10.1038/nrc.2017.35

Cellosaurus cell line OV-90 (CVCL_3768). (n.d.). Cellosaurus. Retrieved February 16, 2023, from https://www.cellosaurus.org/CVCL_3768

Ceasar, S. A., Rajan, V., Prykhozhij, S. V., Berman, J. N., & Ignacimuthu, S. (2016). Insert, remove or replace: A highly advanced genome editing system using CRISPR/Cas9. Biochimica et biophysica acta, 1863(9), 2333–2344. https://doi.org/10.1016/j.bbamcr.2016.06.009

Chakroborty, D., Emani, M. R., Klén, R., Böckelman, C., Hagström, J., Haglund, C., Ristimäki, A., Lahesmaa, R., & Elo, L. L. (2019). L1TD1 - A prognostic marker for colon cancer. BMC Cancer, 19(1). https://doi.org/10.1186/s12885-019-5952-2

Chiu, C. C., Huang, W. C., Lee, K. D., Chen, C. C., Hsu, C. C., Kang, M. L., ... & Hsiao, S. H. (2017). Loss of L1TD1 suppresses Notch1 induced LINE1 methylation and genomic stability. Cancer Research, 77(13_Supplement), 2409-2409. https://doi.org/10.1158/1538-7445.AM2017-2409

Cordaux, R., & Batzer, M. A. (2009). The impact of retrotransposons on human genome evolution. In Nature Reviews Genetics (Vol. 10, Issue 10, pp. 691–703). https://doi.org/10.1038/nrg2640

Emani, M. R., Närvä, E., Stubb, A., Chakroborty, D., Viitala, M., Rokka, A., Rahkonen, N., Moulder, R., Denessiouk, K., Trokovic, R., Lund, R., Elo, L. L., & Lahesmaa, R. (2015). The L1TD1 protein interactome reveals the importance of post-transcriptional regulation in human pluripotency. Stem Cell Reports, 4(3). https://doi.org/10.1016/j.stemcr.2015.01.01 HYPERLINK "https://doi.org/10.1016/j.stemcr.2015.01.014"4

Ewing, A.D., Ballinger, T.J., Earl, D. *et al.* Retrotransposition of gene transcripts leads to structural variation in mammalian genomes. Genome Biol 14, R22 (2013). https://doi.org/10.1186/gb-2013-14-3-r22

Expression of L1TD1 in cancer - Summary. (n.d.). The Human Protein Atlas. Retrieved March 16, 2023, from https://www.proteinatlas.org/ENSG00000240563-L1TD1/pathology

Fernández, C. R. (2021, November 3). CRISPR-Cas9: The Gene Editing Tool Changing the World. Labiotech. Retrieved February 16, 2023, from https://www.labiotech.eu/in-depth/crispr-cas9-review-gene-editing-tool/

Green, M. R., & Sambrook, J. (2019). Nested Polymerase Chain Reaction (PCR). Cold Spring Harbor protocols, 2019(2), 10.1101/pdb.prot095182. https://doi.org/10.1101/pdb.prot095182

Holschbach, M. (n.d.). Western Blot: Gelelektrophorese für Proteine. Antikoerper-Online.de. Retrieved February 7, 2023, from https://www.antikoerper-online.de/resources/17/1224/western-blot-gelelektrophorese-fuer-proteine/

Kaneko-Ishino, T., & Ishino, F. (2012). The role of genes domesticated from LTR retrotransposons and retroviruses in mammals. In Frontiers in Microbiology (Vol. 3, Issue JUL). Frontiers Research Foundation. https://doi.org/10.3389/fmicb.2012.002

Key Takeaways from the HGR Practice in China (Part A). (2022, December 8). Lexology. Retrieved March 29, 2023, from https://www.lexology.com/library/detail.aspx?g=ccefae35-3736-4f48-88b7-9e37788593df
62

Kumar G. (2018). Principle and Method of Silver Staining of Proteins Separated by Sodium Dodecyl Sulfate-Polyacrylamide Gel Electrophoresis. *Methods in molecular biology (Clifton, N.J.)*, *1853*, 231–236. https://doi.org/10.1007/978-1-4939-8745-0_26

McKerrow, W., Kagermazova, L., Doudican, N., Frazzette, N., Kaparos, E. I., Evans, S. A., Rocha, A., Sedivy, J. M., Neretti, N., Carucci, J., Boeke, J. D., & Fenyö, D. (2023). LINE-1 retrotransposon expression in cancerous, epithelial and neuronal cells revealed by 5' single-cell

RNA-Seq. Nucleic acids research, gkad049. Advance online publication. https://doi.org/10.1093/nar/gkad049

McLaughlin, R. N., Jr, Young, J. M., Yang, L., Neme, R., Wichman, H. A., & Malik, H. S. (2014). Positive selection and multiple losses of the LINE-1-derived L1TD1 gene in mammals suggest a dual role in genome defense and pluripotency. PLoS genetics, 10(9), e1004531. https://doi.org/10.1371/journal.pgen.1004531

Misiak, B., Ricceri, L., & Sąsiadek, M. M. (2019). Transposable Elements and Their Epigenetic Regulation in Mental Disorders: Current Evidence in the Field. Frontiers in genetics, 10, 580. https://doi.org/10.3389/fgene.2019.00580

Mita, P., & Boeke, J. D. (2016). How retrotransposons shape genome regulation. Current opinion in genetics & development, 37, 90–100. https://doi.org/10.1016/j.gde.2016.01.001

Mita, P., Wudzinska, A., Sun, X., Andrade, J., Nayak, S., Kahler, D. J., Badri, S., LaCava, J., Ueberheide, B., Yun, C. Y., Fenyö, D., & Boeke, J. D. (2018). LINE-1 protein localization and functional dynamics during the cell cycle. eLife, 7, e30058. https://doi.org/10.7554/eLife.30058

Montoliu, L., Montoliu, L., & Mojica, F. (n.d.). *The CRISPR web page*. CNB - Centro Nacional de Biotecnología. Retrieved August 1, 2023, from http://wwwuser.cnb.csic.es/~montoliu/CRISPR/

Muñoz-López, M., & García-Pérez, J. L. (2010). DNA transposons: nature and applications in genomics. Current genomics, 11(2), 115–128. https://doi.org/10.2174/138920210790886871

Närvä, E., Rahkonen, N., Emani, M. R., Lund, R., Pursiheimo, J. P., Nästi, J., Autio, R., Rasool, O., Denessiouk, K., Lähdesmäki, H., Anjana, R., & Lahesmaa, R. (2012). RNA-binding protein L1TD1 interacts with LIN28 via RNA and is required for human embryonic stem cell self-renewal and cancer cell proliferation. Stem Cells, 30(3). https://doi.org/10.1002/stem.1013

Negritto, M. C. (n.d.). Repairing Double-Strand DNA Breaks. Nature Education 3(9):26. Retrieved 03 22, 2023, from https://www.nature.com/scitable/topicpage/repairing-double-strand-dna-breaks-14432332/

NCBI (n.d.). National Center for Biotechnology Information. Retrieved June 11, 2023, from https://www.ncbi.nlm.nih.gov/

OLS Ontology Research. EMBL-EBI (n.d.). HAP-1. Retrieved March 29, 2023, from https://www.ebi.ac.uk/ols/ontologies/efo/terms?short_form=EFO_0007598

Pace, J. K., 2nd, & Feschotte, C. (2007). The evolutionary history of human DNA transposons: evidence for intense activity in the primate lineage. Genome research, 17(4), 422–432. https://doi.org/10.1101/gr.5826307

Pink, R. C., Wicks, K., Caley, D. P., Punch, E. K., Jacobs, L., & Carter, D. R. (2011). Pseudogenes: pseudo-functional or key regulators in health and disease?. RNA (New York, N.Y.), 17(5), 792–798. https://doi.org/10.1261/rna.2658311

Pfaffl, M. W. (2001). A new mathematical model for relative quantification in real-time RT-PCR. Nucleic acids research, 29(9), e45. https://doi.org/10.1093/nar/29.9.e45

Pratt, A. J., & MacRae, I. J. (2009). The RNA-induced silencing complex: a versatile gene-silencing machine. The Journal of biological chemistry, 284(27), 17897–17901. https://doi.org/10.1074/jbc.R900012200

Ran, F., Hsu, P., Wright, J. *et al.* (2013) Genome engineering using the CRISPR-Cas9 system. Nat Protoc 8, 2281–2308. https://doi.org/10.1038/nprot.2013.143

Rio, D. C., Ares, M., Jr, Hannon, G. J., & Nilsen, T. W. (2010). Purification of RNA using TRIzol (TRI reagent). *Cold Spring Harbor protocols*, *2010*(6), pdb.prot5439. https://doi.org/10.1101/pdb.prot5439

Rice, D., & Galbraith, M. (2008, November 16). .,. ., - YouTube. Retrieved April 3, 2023, from https://www.nature.com/articles/nprot.2006.288

RNA immunoprecipitation chip. (n.d.). Wikipedia. Retrieved February 10, 2023, from https://en.wikipedia.org/wiki/RNA_immunoprecipitation_chip

Santos, M. C. T., Silva, P. B. G., Rodini, C. O., Furukawa, G., Marco Antonio, D. S., Zanotto-Filho, A., Moreira, J. C. F., & Okamoto, O. K. (2015). Embryonic Stem Cell-Related Protein L1TD1 Is Required for Cell Viability, Neurosphere Formation, and Chemoresistance in Medulloblastoma. Stem Cells and Development, 24(22). https://doi.org/10.1089/scd.2015.0052

Shapiro J. A. (2014). Epigenetic control of mobile DNA as an interface between experience and genome change. Frontiers in genetics, 5, 87. https://doi.org/10.3389/fgene.2014.00087

Sun, Z., Zhang, R., Zhang, X. *et al.* LINE-1 promotes tumorigenicity and exacerbates tumor progression via stimulating metabolism reprogramming in non-small cell lung cancer. Mol Cancer 21, 147 (2022). https://doi.org/10.1186/s12943-022-01618-5

The principle and method of immunoprecipitation (IP). (n.d.). The principle and method of immunoprecipitation (IP) | MBL Life Science -JAPAN-. Retrieved July 4, 2023, from https://ruo.mbl.co.jp/bio/e/support/method/immunoprecipitation.html

Tissue expression of L1TD1 - Summary. (n.d.). The Human Protein Atlas. Retrieved June 2, 2023, from https://www.proteinatlas.org/ENSG00000240563-L1TD1/tissue#expression_cluster

Tissue expression of L1TD1 - Summary. (n.d.). The Human Protein Atlas. Retrieved July 3, 2023, from https://www.proteinatlas.org/ENSG00000240563-L1TD1/tissue

Underwood, C. J., Henderson, I. R., & Martienssen, R. A. (2017). Genetic and epigenetic variation of transposable elements in Arabidopsis. Current opinion in plant biology, 36, 135–141. https://doi.org/10.1016/j.pbi.2017.03.002

Vítor, A. C., Huertas, P., Legube, G., & de Almeida, S. F. (2020). Studying DNA Double-Strand Break Repair: An Ever-Growing Toolbox. Frontiers in molecular biosciences, 7, 24. https://doi.org/10.3389/fmolb.2020.00024

V5-Tag: Properties. (n.d.). Proteintech. Retrieved April 6, 2023, from https://www.ptglab.com/news/blog/v5-tag-properties/

What is Mass Spectrometry? (n.d.). Broad Institute. Retrieved June 17, 2023, from https://www.broadinstitute.org/technology-areas/what-mass-spectrometry

Wong, R. C., Ibrahim, A., Fong, H., Thompson, N., Lock, L. F., & Donovan, P. J. (2011). L1TD1 is a marker for undifferentiated human embryonic stem cells. PloS one, 6(4), e19355. https://doi.org/10.1371/journal.pone.0019355

Jangam, D., Feschotte, C., & Betrán, E. (2017). Transposable Element Domestication As an Adaptation to Evolutionary Conflicts. In Trends in Genetics (Vol. 33, Issue 11, pp. 817–831). Elsevier Ltd. https://doi.org/10.1016/j.tig.2017.07.011

Xiao-Jie, L., Hui-Ying, X., Qi, X., Jiang, X., & Shi-Jie, M. (2016). LINE-1 in cancer: Multifaceted functions and potential clinical implications. In Genetics in Medicine (Vol. 18, Issue 5). https://doi.org/10.1038/gim.2015.119

Zhang, X., Zhang, R., & Yu, J. (2020). New Understanding of the Relevant Role of LINE-1 Retrotransposition in Human Disease and Immune Modulation . In Frontiers in Cell and Developmental Biology (Vol. 8). https://www.frontiersin.org/article/10.3389/fcell.2020.00657